2017

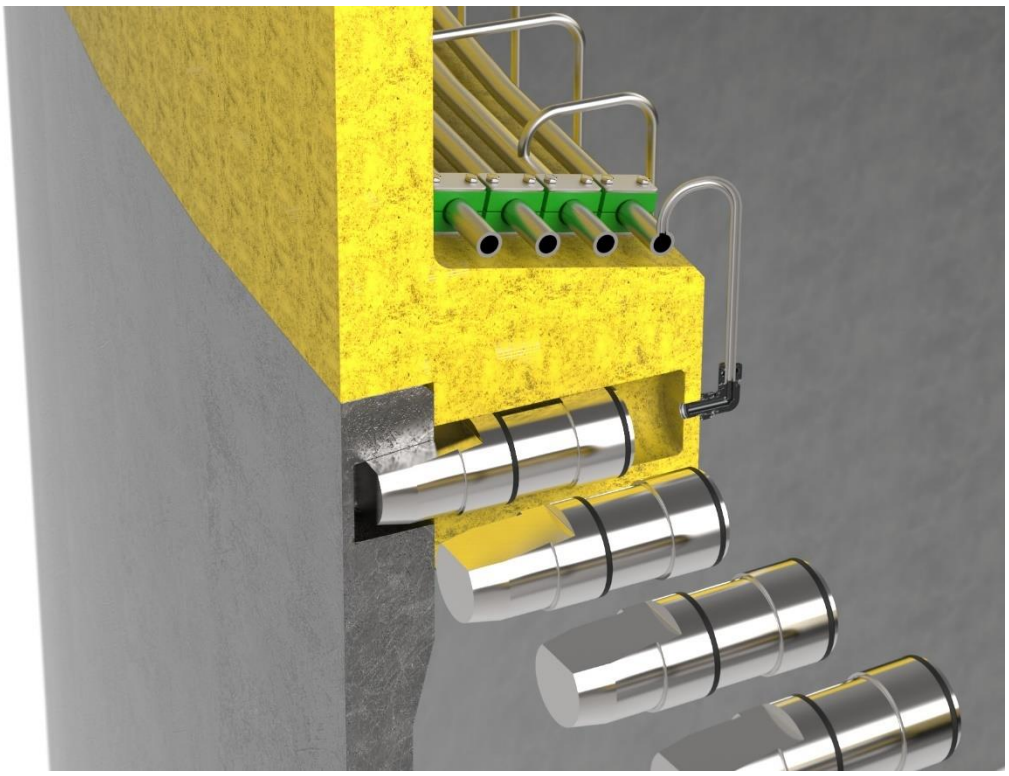

Design and analysis of a wedge connection for offshore foundations

K.E.Y. Creusen

TU Delft

FISTUCA

Design and analysis of a wedge connection for offshore foundations

By

K.E.Y. Creusen

in partial fulfilment of the requirements for the degree of

Master of Science

in Offshore and Dredging Engineering

at the Delft University of Technology,

to be defended publicly on Monday November 6, 2017 at 15:00.

Supervisor:	Prof. dr. M. V. Veljkovic	TU Delft
Thesis committee:	Ir. M.L.A. Segeren	TU Delft
	Dr. F. Pisanó	TU Delft
	Ir. J. Winkes	Fistuca B.V.

Abstract

The offshore wind industry is developing larger turbines, often placed in deeper water. This requires larger foundations. The predominant foundation type is the steel monopile, typically consisting of two large diameter pipes, the monopile (MP) and the transition piece (TP). The Wedge Connection is a new type of connection between these components which is investigated and designed in this thesis. The core of the wedge connection is a dowel with an inclined plane on one end. A large number of these dowels is placed around the circumference in a flange fitted to the TP. Holes with an inclined plane matching the dowel are machined into an MP flange. During installation, the TP is placed on top of the MP and the holes and dowels are aligned. The dowels are displaced horizontally with a hydraulic system. The hydraulic pressure is converted into a vertical preload through the inclined plane.

In a comparison of connection concepts the strengths and weaknesses of the wedge connection with regards to other concepts are found. Two options are currently on the market, grouting and bolted flanges. Grouted connections have proven susceptible to long-term degradation, while bolted flanges have limited scalability and can be applied above the waterline only. The main benefits of the wedge connection are the option to apply it under water and the fact that no significant overlap is required. This makes the wedge connection a commercially attractive option.

The fundamental principle of the wedge connection is a vertical preload generated through an inclined plane. This allows a tensile load on a segment of the connection (caused by the bending moment in the foundation) to be transferred to the foundation via two load paths: by decreasing the preload, and by loading the dowel itself in shear.

In a set of analytical equations the sensitivity to the wedge angle and friction coefficient is investigated. Based on these equations and the shear strength of the dowel, a preliminary design is drafted for a hypothetical foundation with 10 m diameter.

This design is modelled using ANSYS APDL. The connection is incrementally loaded up to the ultimate tensile load. A study is performed on the behaviour of the connection. The sensitivity of the connection to factors such as friction coefficient, input pressure and small geometry changes is considered.

The wedge connection has been shown to be a viable concept for connecting offshore wind turbine foundations. Further investigation into the frictional properties, material combinations and fatigue life is recommended to further mature the concept.

Acknowledgements

I would like to thank a number of people for their continuous support, recommendations and critical review of my work:

prof. Milan Veljkovic, whose enthusiasm about the concept has inspired me to keep going, and Maxim Segeren, who never failed to guide my thought process in the right direction.

Jasper Winkes, for allowing me to develop his idea from a back-of-the-envelope sketch to where we are now, and enabling conversations with a network of professionals which guided the project.

The entire team at Fistuca, even though we have been working on completely different projects, for providing me with perspective, interesting ideas at the whiteboard and many great lunchtimes. I am excited to join this team, and see the hammer come together!

Maarten Vogel, MC Anderson and most recently Lena Bakaloni with whom I have shared the 'intern table' in the office, where many software-related frustrations were shared, easy and complex problems were solved and new ideas came to light.

Finally, thanks to my parents, who have always encouraged me to think for myself, and supported my plans and ideas, and especially to Anouk, for keeping my feet on the ground and my head up high during these months.

Delft, 26-10-2017 *Koen Creusen*

Contents

LIST OF TABLES

SYMBOLS AND UNITS

α	Inclined plane angle of the wedge	[°]
f	Fraction of load transferred	[-]
h_{fluid}	Lubricating fluid thickness	[m]
I	Second area moment of inertia	[m^4]
k	c-t-c spacing of dowels	[D_{dowel}]
k_d	Dowel stiffness	[N/m]
k_j	Joint stiffness	[N/m]
k_{normal}	Contact stiffness FE model	[N/m]
λ	Additional contact term FE model	[N]
μ	Friction coefficient	[-]
N	Number of cycles	[-]
P	Preload on the MP/TP interface	[N]
R_a	Surface roughness	[m]
S	First moment of inertia	[m^3]
σ_y	Yield stress of material	[N/m^2]
θ	Internal angle inclined plane width	[°]
V	Shear load	[N]

1 Introduction

1.1 Offshore wind industry trends

Offshore wind farms are increasingly being developed with larger wind turbines, placed in deeper waters. This leads to heavier foundations with larger diameters (WindEurope 2017). The monopile is still the dominant foundation type, but jackets are applied at the deepest locations. However, as fabricators are now able to produce monopile foundations of up to 11 m diameter and masses up to 2000 tons (Seidel 2014, Sif Offshore Foundations 2017), the limit to foundation size seems to be installation capacity. Numerous current projects are using large monopiles in water depths of ca. 40 m with the largest available turbines (>7 MW), for example the EnBW Albatros windpark (Sif Offshore Foundations 2017b).

1.1.1 Connections in monopile foundations

Most modern monopile foundations consist of two components: the monopile (MP), which is driven into the seabed and typically extends a few meters above mean sea level (MSL), and the transition piece (TP), which extends from the top of the MP to the bottom of the turbine tower, typically ca. 20 m above MSL. The MP/TP connection was formed by a grout skirt in the first monopile foundations. This design was taken from the offshore oil and gas industry practice, where piles are grouted to jacket legs. In 2009 a number of failures of grouted connections occurred, and the industry sought an alternative (Dallyn et al. 2015). The current standard practice is to apply very large flanges to the MP and TP, which are bolted together with bolts of up to M72 size. The alignment, torqueing and maintenance of such a bolted connection is currently done manually with hydraulic tools.

1.2 The wedge connection

In response to the issues with grout, and the installation and maintenance cost associated with bolted connections, a novel connection method has been developed at Fistuca. This connection uses the principle of the inclined plane to achieve a preload on flanges fixed to the MP/TP, similar to the bolted connection. The inclined plane, or wedge, is applied to the underside of the MP flange, and to a radially displaceable dowel (Figure 1).

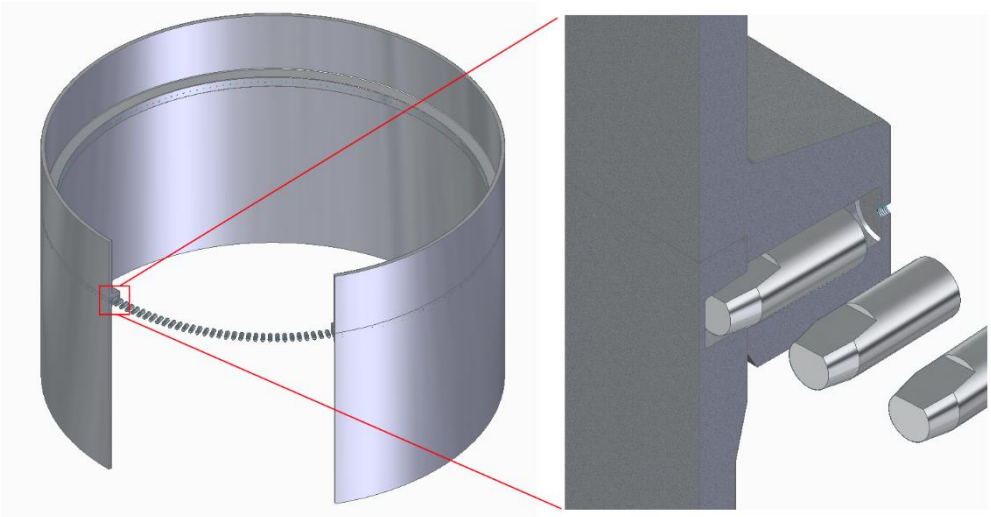

Figure 1 - Overview of the wedge connection

The installation of the wedge connection is its main strength. The TP can be lifted and rested on the MP flange. No exact alignment is required. The dowel is radially displaced by hydraulics, until it comes into contact with the matching inclined plane of the MP flange (Figure 2). Hydraulic pressure on the backside of the dowel is translated to vertical preload on the connection via the inclined plane. Once the desired preload is achieved, the connection is complete. No personnel is required at the connection level, so the connection can be made underwater or in awkward locations. This makes it also an interesting alternative for connections in turbine towers. An underwater connection allows for a more even distribution of length and mass between the MP and TP. This allows the installation of larger foundations with relatively small vessels. An additional benefit is that the dowels can be used for seafastening of the TP to the deck of an installation vessel. An overview of possible locations for the connection in an MP foundation is presented in Figure 3.

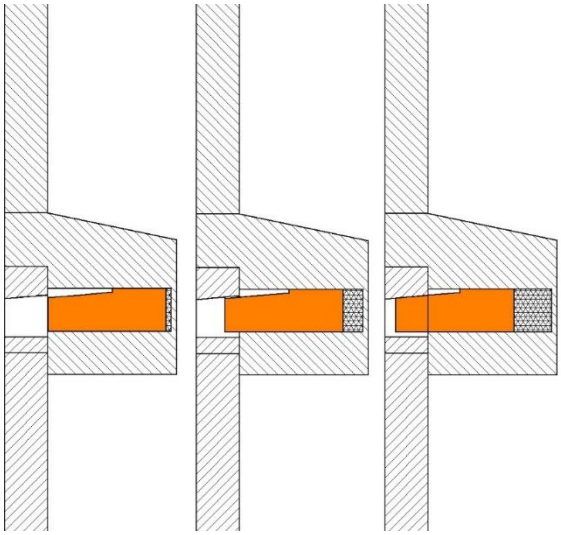

Figure 2 - Installation by hydraulics

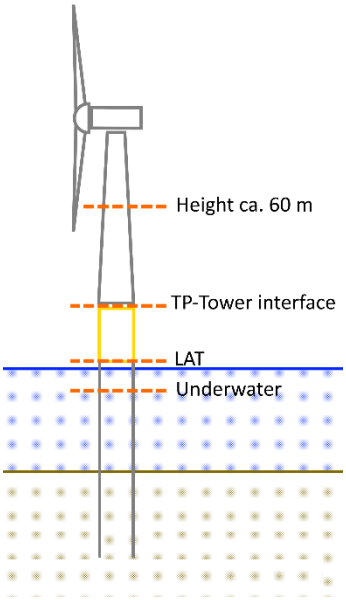

Figure 3 - Possible connection locations

1.3 Design goal and research questions: understanding contact

The final goal of this thesis is to investigate the principles of the wedge connection, to make a preliminary design, and to understand the sensitivity of this connection to various design parameters. The key principle of the connection is steel-on-steel contact. To understand this mechanism and develop a design, the following research questions are to be answered:

1) What are the (dis)advantages of the wedge connection, compared to other connection methods for offshore wind foundations?
   a) Considering technical feasibility;
   b) Material cost;
   c) Manufacturing;
   d) Installation;
   e) Serviceability.
2) What are the requirements that the connection needs to satisfy?
3) What is the load transfer path of the wedge connection?
   a) What is the mechanism and magnitude of friction along the dowel?
4) How can the contact surfaces be modelled, both analytically and numerically?

5) How can the friction mechanism be modelled, both analytically and numerically?
6) How does the connection behave under ULS loading?
7) How does this behaviour change if any of the design parameters is changed (e.g. input pressure, friction coefficient)?

1.4 Approach and report outline

The starting point is the concept of the wedge connection, as introduced in section 1.2. The end goal is to develop a validated initial design for a 10 m diameter monopile foundation, where the connection is made below MSL.

First of all, the concept of the wedge connection is compared to other connection methods for large-diameter offshore tubulars. This is to gain understanding on the key advantages of the wedge connection, and to identify challenges that need to be considered in the design. A literature review will provide insight into the details of the various connection methods available. This leads to a qualitative comparison on a number of criteria that are important in offshore engineering. In this way the (dis)advantages of the wedge connection can be identified. This review and comparison can be found in chapter 2.

To make a design, the connection needs to modelled. Initially, this model will be analytical to understand the load path and frictional mechanisms that form the connection. Research into the nature of contact surfaces and frictional mechanisms is required as input for these calculations. The research questions 2 - 5 posed in 1.3 are answered in chapter 0.

Using this knowledge on the principles of the wedge connection, a preliminary design can be drafted (chapter 0). The goal is to fix design parameters such as the wedge angle and the number of dowels, and to assign dimensions to the connection, based on the previous analysis. First the design requirements must be stated; this includes the imposed loads and requirements on the behaviour of the connection.

Based on this initial design and requirements, a FE model is developed in chapter 5. First the numerical part of questions 4 and 5 will be answered, to incorporate contact surfaces and friction into the FE model. A simplified version of the FE model is used to validate it against the analytical results. The model is used for more detailed analysis of the behaviour of the wedge connection under ULS loads. This model also allows for a parameter sensitivity study.

The end result is a validated, preliminary design of the wedge connection for a monopile foundation. Details to facilitate fabrication and installation are included in a more detailed design, found in chapter 0.

1.5 Fistuca

Fistuca started as a spin-off from Eindhoven University of Technology, developing equipment for the foundation industry. In 2011 the company began developing the BLUE Piling technology, specifically for driving large offshore monopiles. This technology allows for quieter, more powerful pile driving. Larger foundations can be installed for lower cost, as fewer noise reduction measures are required.

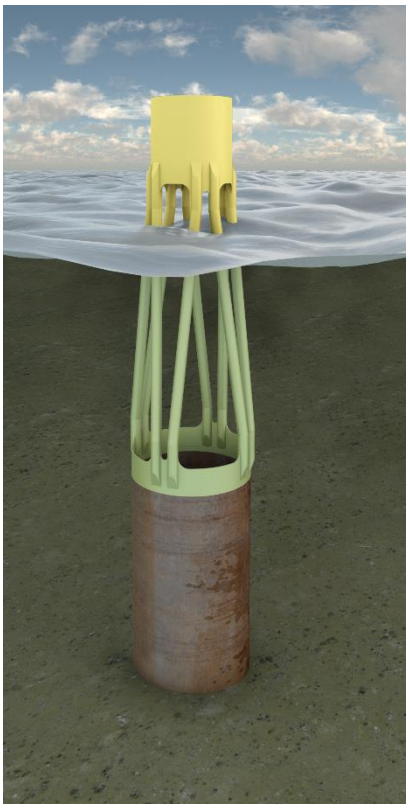

Figure 4 - The Hybrid Monopile

More recently, the company has developed the Hybrid Monopile. This novel foundation concept combines the advantages of jacket and monopile foundations by applying a hydrodynamically transparent, braced section in the wave zone in between monopile shells. This concept could benefit from an underwater connection between the braced and monopile sections, such as the wedge connection.

2 Concept comparison

Two concepts are currently in use for connecting large-diameter tubulars offshore: grouting and bolting. In the context of offshore wind turbine substructures, especially monopile-transition piece (MP-TP) connections, both of these methods have significant drawbacks. In response a new connection method based on slip joints has been developed. A variant, the double slip joint is also currently under investigation. Further alternatives that have been proposed include tension-free, eccentric-free and friction bolted connections.

In this chapter, these seven concepts are introduced and assessed. A qualitative multi-criteria analysis is performed to investigate the properties of these connection methods and compare them to the wedge connection. The key advantages and challenges for the wedge connection are identified.

2.1 Criteria

To investigate the benefits and downsides of each connection concept, several criteria can be used. These criteria have been defined based on the industry priorities: safety and cost. Safety, from a technical point of view, can be defined as the requirement for the structure to withstand all loads it will encounter in its lifetime. The other priority is cost, as foundations account for a large (>15 %) fraction of offshore wind cost (Voormolen, Junginger, and van Sark 2016). Furthermore the offshore wind industry is quickly moving to larger turbines and foundations, so a connection concept should also be feasible at larger diameters. Based on these priorities, the following criteria have been selected:

- **Technology Readiness Level** (TRL). To estimate the maturity of various concepts, the TRL definitions as established for the Horizon 2020 programme are used (European Commission 2017). These are repeated in Table 1.

  Table 1 - Technology Readiness Levels (TRLs), taken from European Commission 2017

TRL 1	Basic principles observed
TRL 2	Technology concept formulated
TRL 3	Experimental proof of concept
TRL 4	Technology validated in lab
TRL 5	Technology validated in relevant environment
TRL 6	Technology demonstrated in relevant environment
TRL 7	System prototype demonstration in operational environment
TRL 8	System complete and qualified
TRL 9	Actual system proven in operational environment

- **Material Cost**. A basic bill of content calculation can show the material cost of each connection concept. The basic structural dimensions are based on a Ø 6 m monopile, with a wall thickness at the connection of 80 mm. All materials that are required for the connection, beyond the primary steel of the MP and TP are incorporated.
- **Manufacturing**. The materials, dimensions and tolerances required for the design largely determine the manufacturing cost.
- **Installation**. Offshore work is expensive, especially if it involves special vessels. The ability to correct verticality is mentioned here.
- **Serviceability**. If a connection method requires offshore inspection and/or servicing during its lifetime, this will lead to significant Operations & Maintenance

(O&M) costs. The susceptibility of the connection method to corrosion, and measures to prevent corrosion, are mentioned here as well.

- **Scalability**. The offshore wind sector is quickly moving to larger monopiles of up to 10 meters in diameter. Therefore an additional point of comparison is how to concept scales up to larger diameters in relation to materials and technical feasibility. This can be expressed qualitatively in general statements, and quantitative with the factor with which the material use scales with the diameter.
- **Underwater**. To more evenly distribute length and mass between the MP and TP of an offshore wind foundation, it has been suggested to make an underwater connection. This would also benefit the Hybrid Monopile concept, as the braced section could be installed separately from the main monopile.

Besides analysing the various connection concepts on these seven criteria, the following section will also include a short introduction on the development and load transfer path of each concept. Many of the criteria come with some degree of subjectivity. Therefore the value of each concept has been discussed with a number of industry experts from academia, engineering firms, contractors and utilities. This section attempts to summarize these views into a general description of connection methods for offshore wind foundations.

2.2 Grouted connection

Jacket structures for the offshore oil and gas industry have been using grout as a connection method for decades. In these structures, foundation piles are inserted through the structure's legs, and connected at the top. Early offshore wind developments adopted this method to connect the TP to the MP (Lotsberg 2013). Grouted connections have been the default connection method until 2009, when unexpected settlements were noticed at several offshore wind farms. Adapted grouted connections, with shear keys, conical steel sections or additional elastomer bearings have been used after that (4C offshore 2013).

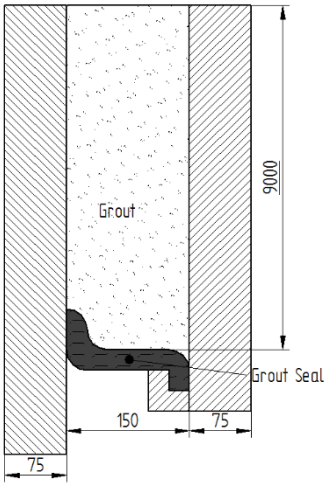

Figure 6 - Typical grouted connection

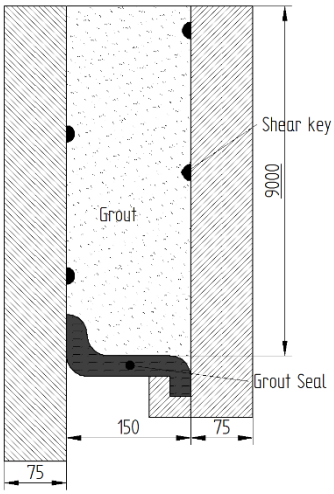

Figure 5 - Typical grouted connection with shear keys

Load transfer path

Wind turbines foundations are more heavily loaded by bending moments than permanent axial load, as the rotor thrust is large and originated at a distance from the foundation.

Horizontal contact pressure provide a load path from TP to MP (blue arrows in Figure 7). Vertical and horizontal friction forces due to contact pressure and surface roughness also contribute to the moment capacity (red and green arrows in Figure 7). This leads to tensile stresses between the grout and steel, which may exceed the tension capacity of the grout.

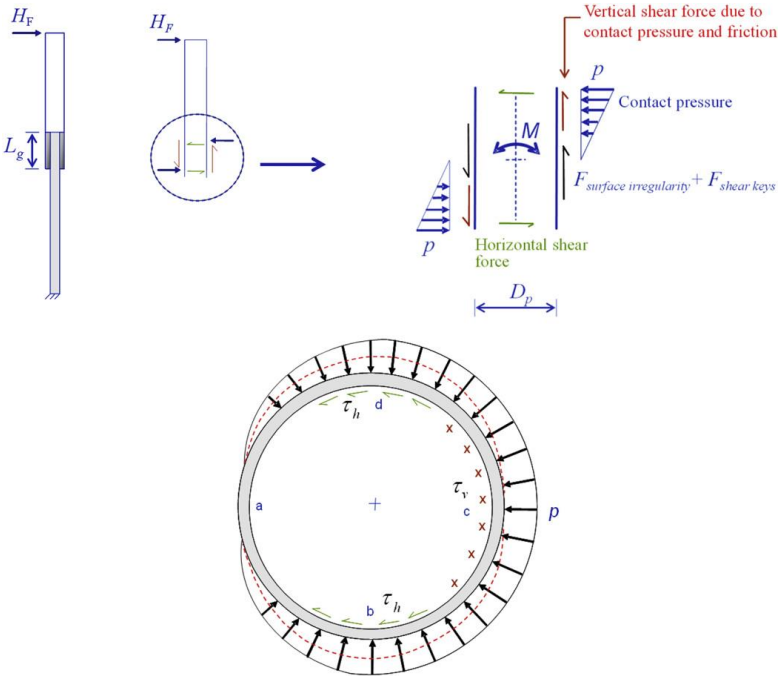

Figure 7 - Reaction forces in the grouted connection (Lotsberg 2013)

As the MP and TP are relatively slender (high diameter to thickness ratio), they will deform radially under bending moment loading. This leads to relative vertical sliding between the two, which could further degrade the grout (Lotsberg 2013)

To alleviate these issues, horizontal shear keys have been introduced in grouted connections between MP and TP. These shear keys introduce additional moment resistance, and thus (for the same load), decreasing the contact pressure otherwise required. It has been observed that diagonal compressive struts form between shear keys on the TP and shear keys on the MP when the TP moves vertically relative to the MP. In accordance, tension stresses occur in the direction normal to these compressive struts, which will lead to cracking parallel to the compressive strut.

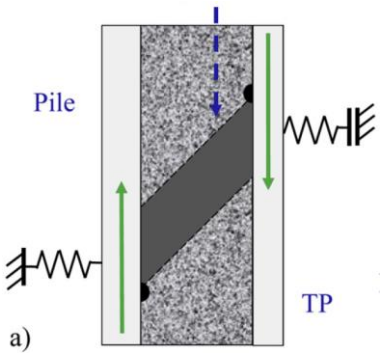

Figure 8 - Compressive strut in grout connection (Lotsberg 2013)

Criteria
TRL

Grouting has been the default method for connection TP's to MP's in the early days of offshore wind energy. In 2009 it came to light many of these connection have insufficient long-term axial capacity, which lead to expensive repair works on many turbines (Dallyn et al. 2015). Two Joint Industry Projects (JIP) were set up, to investigate the structural capacity of grouted joints in offshore wind applications (Lotsberg et al. 2012). In the first project it was assessed that grouted connections without shear keys could no longer be recommended due to the low long-term axial capacity. The second JIP aimed to develop design equations for grouted joints with shear keys. Recommendations based on the projects have been incorporated in the latest design standards, such as DNV-OS-J101.

The system has extensively been proven in the operational environment, thus TRL 9 has been achieved, despite the aforementioned issues.

Material

There is a considerable amount of extra material required for a grouted joint, as the steel of the MP and the TP overlap. A bill of content (BoC) has been drafted for a typical foundation design, see Table 2. A typical grouted connection has an overlap length of the TP over the MP of around $1.5D$. The thickness of the grout itself is taken as $150\ mm$. Additionally, some smaller parts are required for installation purposes: guiding brackets and rubber seals to keep the grout in place before it is hardened. These are estimated at €5000 per connection.

Table 2 - Bill of content grouted connection

Item	Quantity	Unit	€/unit	€ x 1000
Overlap steel	104	t		
Grout	25	m^3		
Additional parts	-	-		
Total				

**Values of 1.5 to 2 €/kg have been quoted for MP/TP steel, for vertical/conical sections.*

Manufacturing

A grouted connection is quite easy in terms of fabrication. The monopile can just be plain steel, while the majority of the additional steel required is simply another section on the TP. A ring has to fabricated and fitted to the bottom of the TP to hold the rubber seal in place. Some (guiding) brackets are required for temporary support of the TP before the grout is cured. Shear keys and/or tapers slightly complicate fabrication.

Installation

The installation of a grouted joint is straightforward, but time consuming. After the MP is hammered into the soil, the TP can be lifted on top. The TP rests on temporary guiding brackets, while personnel is transferred from the vessel to the TP to connect the grouting lines. The grout is pumped from the installation vessel until it is filled to the required level. The verticality of the TP can be corrected via jacks if required. The grout has to cure before it can take any load. Grout curing times increase with decreasing temperature, and can take up to 24 hours before the grout can take wave loads (Sika n.d.). The curing time to reach specified strength is typically quoted as 28 days. This implies that the offshore construction of the rest of the turbine may have to wait.

Serviceability

Once a grouted joint is cured, it is very hard to monitor, as the grout is sandwiched between the MP and TP steel. Typically no service is required. However, if there is a problem with the joint, as was the case in many early offshore wind farms, it will only be identified once the turbine starts settling, which is a major risk. Repairing a failed joint requires extensive additional offshore work (Sabine Lankhorst 2015).

A grouted connection is not particularly sensitive to corrosion. If the grout fails however, water could come in contact with non-corrosion protected steel. This could worsen the condition of the connection.

Scalability

There has been no specific research into using grout for very large diameters. Because of the overlap length given as a factor of D, the material use scales with a factor D^2.

Underwater

Grouted joints are routinely used underwater. Typically the seawater is kept out of the connection by a seal, that also retains the grout while it is curing.

2.3 Bolted connection

A bolted flange is a basic connection method for steel structures. There is extensive experience with smaller scale bolt-flange connections, which are governed by Eurocode 3 (European Committee for Standardization 2005). These connections are typically used in the tower supporting the nacelle in both on- and offshore wind developments. The first offshore wind farm to apply this connection was at the substructure level was the Scroby Sands project in the UK. The turbine tower was directly connected to the monopile foundation, without using a transition piece. Since the grouting issues of ca. 2009, more and more wind farms are moving towards using a bolted connection at the MP/TP interface. Currently bolted flange connections are the industry standard, for both MP/TP and tower section connections.

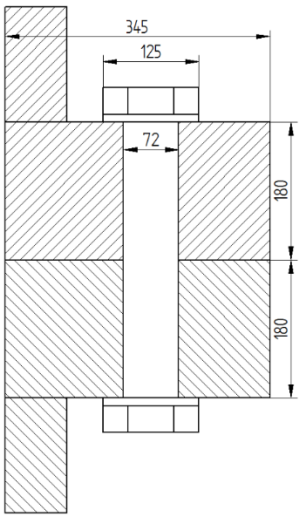

Figure 9 - Typical bolted connection

Load transfer path

Compressive axial loads are simply transferred from shell to shell, while tensile loads are transferred via the prestressed bolts and the flanges. Bolts are prestressed to 70% of their tensile capacity, to bond the ring flanges together (GL 2012). This allows for the majority of the tensile load to be transferred via the flange connection, with a small fraction transferred of the load is carried by the bolt itself. Four failure modes are considered (Petersen, Seidel as cited in (GL 2012)), see also :

- Mode A: Bolt failure
- Mode B: Bolt failure and yielding of flange
- Mode D: Yielding of flange in bolt axis
- Mode E: Yielding of flange under the washer

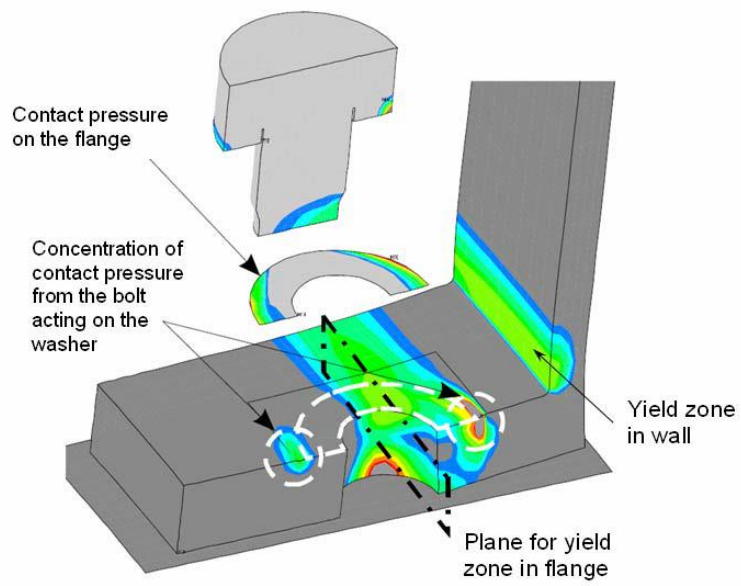

Figure 10 - Bolt-flange connection failure zones (Peter Schaumann, Eichstädt, and others 2015)

In MP-TP connection bolts must be heavily pre-loaded to ensure sufficient capacity, especially for fatigue load cases. Very large bolts are required to achieve this. For the Amrumbank West project (3.6 MW turbine, 5.2 m MP/TP diameter), 96 M72 bolts of grade 10.9 were used.

Criteria

TRL

Bolted flange connection are very common in standard steel structures. The only technical challenge is the scaling to the loads found in offshore wind turbines. This requires very large, high strength bolts and flanges. Nevertheless this type of connection has long been the default in turbine towers, and recently also for MP-TP connections. In 2013 guidelines have been published that allow the use of bolts up to size M72 without additional approval (Gollub et al. 2014). This definitely proved that the technology is at TRL 9.

Material

A bolted flange connection does not require significant amounts of additional material, as the MP and TP have identical diameters, and little to no overlap is required. However, the high strength flanges and bolts required are expensive. A indicative bill of content is presented in Table 3.

Table 3 - Bill of content bolt connection

Item	Quantity	Unit	€/unit	€ x 1000
Forged flange MP/TP steel	18	t		
M72, grade 10.9 bolts	128	-		
Additional sealing material	-	-		
Subtotal				
Option: grout skirt	4	m^3		
Option: grout seal	-	-		
Total				

Manufacturing

The manufacturing of high strength large diameter flanges is a highly specialized task. Only few facilities can provide these flanges at the required strength, dimensions and tolerances. The high strength bolts are somewhat more common. To ensure no water ingress to the MP-TP interface detailed engineering is required. Typically (a combination of) a small, non-load bearing grouted annulus or rubber sealing rings are used. These details complicate fabrication of the TP.

Installation

If a bolted connection is used, the upper part of the MP will be the flange to which the TP will be connected. As the integrity and flatness of this flange is key to the MP-TP connection, it may not deform during piling of the MP. This complicates the piling operation.

When the TP is placed on top of the MP, it must be carefully aligned with the bolt holes. Personnel is transferred to the TP to tighten the bolts. The torque required to achieve correct preload on the bolts is very high, so special hydraulic tools are necessary. The preload is crucial to the connection, so measuring devices are required to monitor the bolt tension during installation (Gollub et al. 2014). The bolted connection is not able to correct any nonverticality of MP installation. If this is an issue, it must be corrected using a shim flange at the TP-tower interface. All in all the installation of a bolted connection is fairly complicated and time consuming.

Serviceability

Classification societies require the bolts to be retightened to specification at least once after commissioning, and regular checks. This requires additional offshore maintenance time, increasing operational expenses. A bolted connection is highly sensitive to corrosion. A small, non-load bearing grouted annulus and/or O-rings are used to prevent water ingress.

Scalability

The material used for a bolted flange connection scales with a factor *D*, which is relatively beneficial. However the size and number of bolts required presents a challenge, for both design and installation. Bolts larger than M72 would need new certification, and are even more difficult to handle and torque.

Underwater

Technically a bolted flange could be applied underwater. The installation of bolts however would need to be done by ROV or divers. This is probably not economically feasible. Furthermore corrosion would be a major issue.

2.4 Slip joint

In response to the issues with grout, and the installation and serviceability issues of bolted connections, the slip joint connection has been proposed. The principle of the slip joint is to slide two conical steel section over each other, without the use any fastening mechanism. (J. Van der Tempel, B Schipholt 2003). The concept was originally developed for onshore wind turbine tower section by the Dutch company WindMaster. Years after the bankruptcy of WindMaster in 1998, the concept was proposed as an alternative to grouted connections at TU Delft in 2003 by Van der Tempel and Lutje Schipholt. The slip joint was one of the subjects of the FLOW joint research programme. The concept has been applied in the onshore demonstrator turbine by DOT. As a result, the connection is currently undergoing certification by DNV (Rolf de Vos 2016).

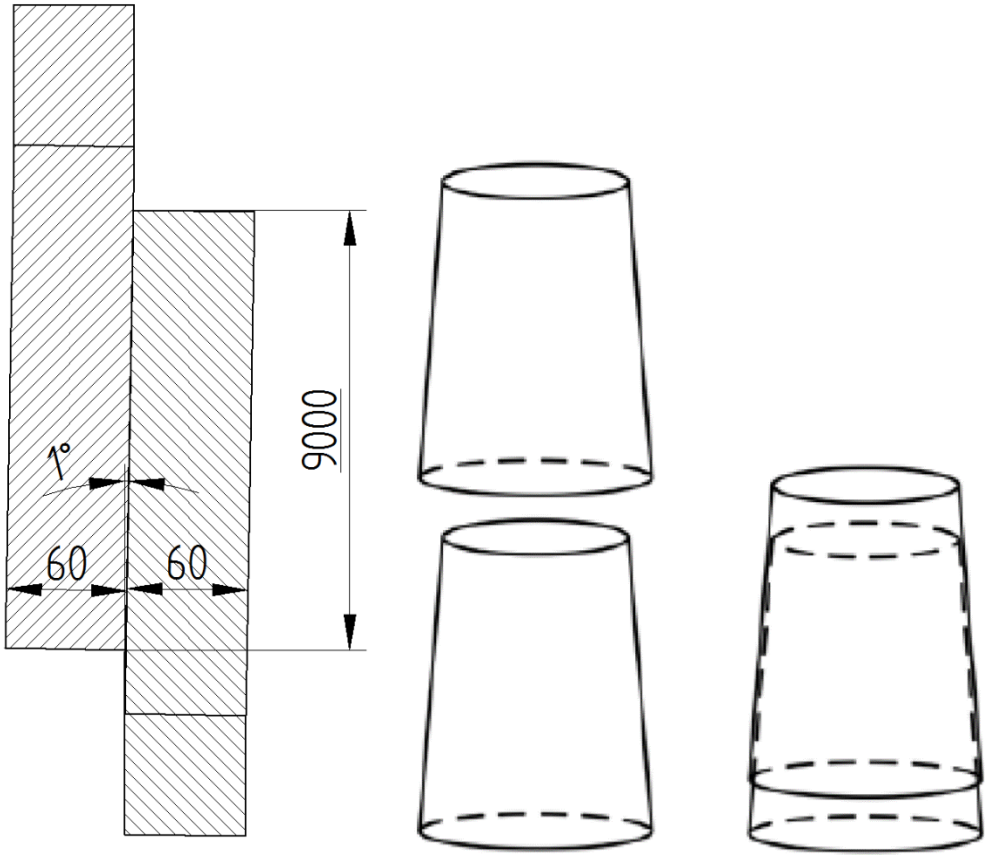

Figure 11 - Typical slip joint – dimensions indicatory

Load transfer path

The load is transferred from the TP to the MP via friction and contact force normal to the connection. Friction is achieved through contact pressure and a certain friction coefficient. Large overlaps of around 1.5D are required to successfully transfer loads (Segeren et al. 2014).

Criteria
TRL

The slip joint has been proven at a limited, onshore scale in the WindMaster and DOT towers. Furthermore 1:10 prototypes have been tested as part of the FLOW programme. Therefore the concept is at TRL 4 or 5, depending on how the onshore demonstrations are valued.

Material

The slip joint requires a significant amount of overlapping, conical steel. Assuming a diameter of 6 m, wall thickness of 80 mm and overlap of 1.8D, and neglecting the small cone angle for the mass calculation, 250 t of structural steel is required. The cost of 125 t of vertical steel is subtracted from the cost calculation, to account for the overlap.

Table 4 - Bill of content slip joint

Item	Quantity	Unit	€/unit	€ x 1000
Overlapping steel	250	t		
Discount vertical steel	-125	t		
Total				

**Here the value of €2/kg is used as the steel must be conical.*

Manufacturing

The general production of primary steel at an small cone angle is no issue for MP/TP fabricators. The tolerances required for the slip joint to work are unknown, and these might be problematic, as any non-smooth surface area may lead to stress concentrations. Such non-smoothness cannot be predicted during design, so it is presumed high accuracy is required. This, combined with the large overlap lengths required makes fabrication significantly more complex.

Installation

In the original, onshore version of the slip joint by WindMaster, the tower sections were assembled by dropping them over a distance of ca. 10 cm (J. Van der Tempel, B Schipholt 2003). This option has also been investigated for the offshore slip joint by Segeren, but dismissed because it would be rather difficult and risky to execute offshore. It was also shown that the required overlap length could not be achieved. Instead, it was proposed to install the TP by applying a vertical harmonic load. The required settlement can be reached by various combinations of amplitudes and frequencies, of the order of 500 kN at 15 Hz. Higher loads and frequencies lead to larger settlements (Segeren et al. 2014). Another option could be to use the mass of the turbine and the wind loading to reach adequate settlement. The slip joint does not allow for correction of verticality of the TP.

Serviceability

In principle, no service is required for the slip joint. It may be desirable to regularly or continuously measure the settlement of the top part. The corrosion behaviour is unknown at this time, and this is a major point to be investigated before the joint can be applied offshore (Rolf de Vos 2016). Due to the nature of the joint, it is presumed that it is sensitive to corrosion, as the joint relies on even contact which will be disturbed if corrosion occurs. Designing a corrosion protection system is fairly straightforward though, as the concept only uses two parts.

Scalability

Because of the overlap required, the material required for the slip joints scales with a factor D^2. Besides this additional material, the slip joint can fairly easily be scaled to larger diameters.

Underwater

The slip joint may be able to be installed underwater. For corrosion protection it would be required to ensure that the connection is either always above or always below the waterline.

2.5 Double slip joint

The double slip joint is a variant of the slip joint examined in section 2.4. It is currently under development at KCI (KCI 2015). This concepts incorporates two sets of steel, conical rings on the MP and TP to achieve a slip joint in two locations. The smaller contact area compared to a 'normal' slip joint may provide a more exact fit (van Gelder, Klaas Boudewijn, n.d.). A variant of the concept has been proposed in which the TP fits *inside* the MP and the connection is made below waterline.

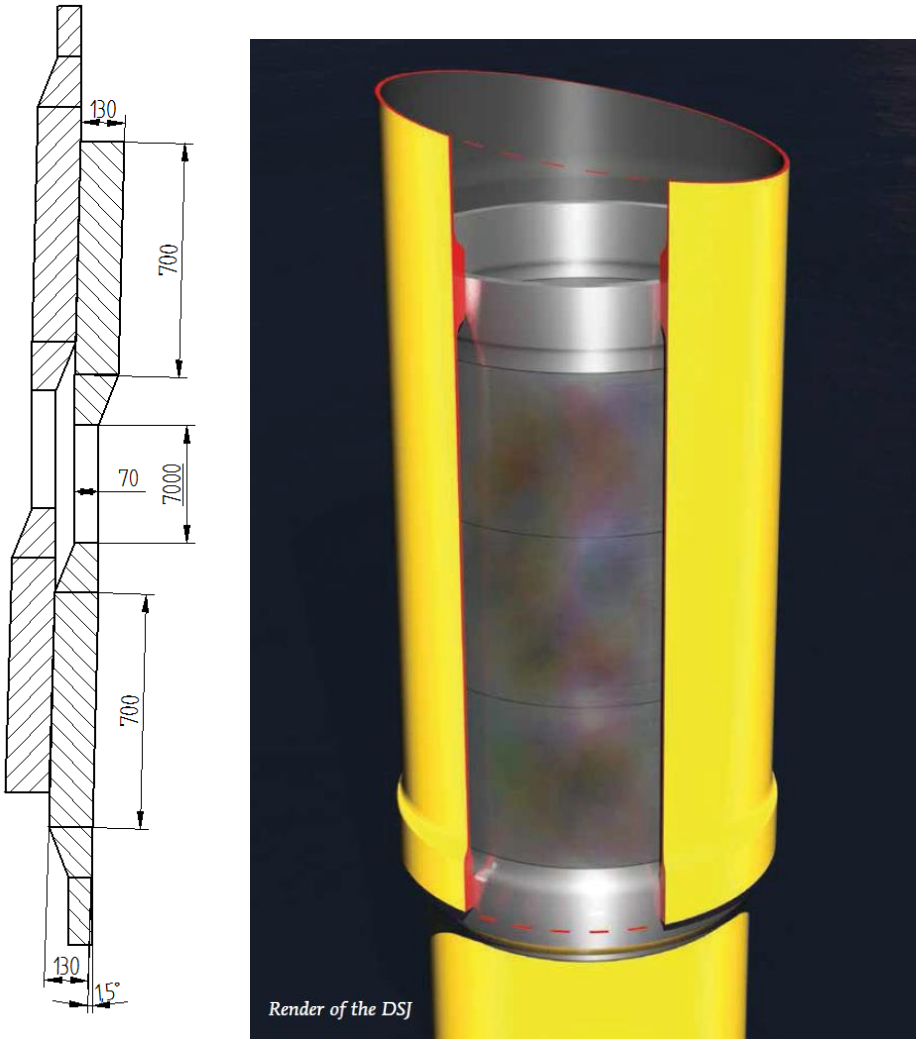

Figure 12 - Typical double slip joint. Dimensions are estimated based on public sketches (KCI 2015)

Load transfer path

The load is transferred via friction and normal contact loads through the contact areas, similar to the normal slip joint. Lower contact forces may be required to transfer moment loads compared the standard slip joint, as the two contact areas are separated vertically.

Criteria

TRL

Little technical information is published on the double slip joint. The most recent public updates suggest that 1:5 scale tests have been conducted with steel components (Van Gelder 2017) . This suggests a TRL of 4.

Material

Two sets of matching steel conical rings form the core of the double slip joint. These are attached to an overlapped section of the TP. The height of each ring is limited to circa 1/4th of its diameter. These rings are made from rolled, forged or expanded steel and must be machined to tight tolerances. Similar to the slip joint the cost of a single section of overlapping steel is removed from the cost calculation.

Table 5 - Bill of content double slip joint

Item	Quantity	Unit	€/unit	€ x 1000
Overlapping steel	167	t		
Conical rings	4*11	t		
Discount vertical steel	-84	t		
Total				

Manufacturing

One of the key challenges of the double slip joint is fabrication. Two sets of closely matching rings must be rolled, forged or expanded, then machined and welded to the TP/MP. Each of these steps must be execute precisely, to ensure even contact pressures.

Installation

The major advantage of the double slip joint is installation, both in time and in complexity. The joint can be installed under self-weight of the TP, settling further once the turbine is installed. No further offshore work is required. In the default double slip joint concept, it is not possible to correct verticality. In the patent application a variant is described where the upper rings are divided in vertically moveable sections, such that the verticality may be corrected. This would add significant complexity to the design.

Serviceability

The location of the interface prevents any normal inspection or maintenance. In principle, neither of these is necessary. The connection is rather sensitive to corrosion, and as such it should be well protected.

Scalability

The DSJ principle is very scalable, and the latest published sketches suggest a diameter of 8 m (Gelder 2016). Due to the required overlap, the material use will scale with a factor of D^2.

This also holds for the height of the machined rings, which will add to the material cost of the concept.

Underwater

Applying the DSJ underwater is one of its main benefits. Corrosion protection might be simplified by the lack of oxygen within the connection as the connection must be very tight.

2.6 Tension-free bolted joint

As an alternative to conventional bolted joints, where the bolts transfer the full tensile load, Schlemenat (1996) has developed a tension-free bolted joint. The original application is industrial pipelines, where thermal expansion and large pressure cycles are very demanding on the joints between pipe section. It has also been proposed to use the tension-free joint in (offshore) wind turbine towers, but this has not been realised.

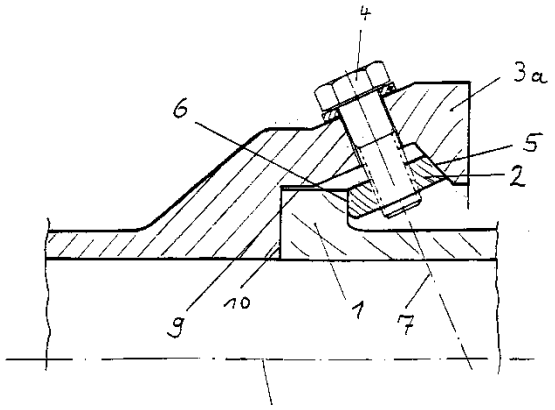

Figure 13 - Schematic of tension-free bolt

Load transfer path

The tension-free joint fixes the connection between two flanges (1 and 3 in Figure 13) by pulling a wedge shaped tensioning nut (2). This ensures that all loads are transferred via contact pressure. The wedge is pulled into the connection by a short bolt (4), that does not transfer any further load, and is thus 'tension-free'.

Criteria

TRL

The concept has been proven in smaller scale applications such as steam generator pipelines. It has not been applied at very large diameters like offshore wind turbines however. This suggest TRL 2, as the two applications are quite different. A major issue is the large overturning moment causing large tension between the flanges. This has to be compensated by a large preload. Achieving this preload via an inclined bolt as in Figure 13 requires high tension in the bolt, partly negating the benefit of the connection.

Material

No reference design is available, as the system has not been applied extensively, and not at all at large diameters. The material cost cannot be estimated realistically. Given the type of flange and bolts, the costs will be larger than a conventional bolted connection.

Manufacturing

A fairly complex flange is required to contain the bolts. The other components are not very complex, but finishing quality on the contact surfaces must be quite high.

Installation

The main steel parts forming the connection can easily be placed on top of each other. To fix the connection, the wedge must be oriented correctly and tightened via a large number of bolts. This prevent underwater application of the connection. Installing the connection above water is more difficult than conventional bolted connections, as the wedge-shaped nut is difficult to access. Correcting non-verticality requires a shim flange, similar to a conventional bolted flange design.

Serviceability

As the bolt itself is not directly part of the load path, it presumably not necessary to maintain it as stringently as conventional bolted connections. Due to the various contact surfaces, the connection is presumably fairly sensitive to corrosion.

Scalability

The concept has the potential to be scalable in a similar manner as a conventional bolted flange connection. However, because no designs are available at the dimensions common in the offshore wind industry, it might be not viable at all.

Underwater

It will be extremely difficult to apply this concept in an underwater connection.

2.7 Eccentric-free bolted joint

A reference was found to a bolted connection that avoids eccentric loading on the bolts (by MECAL (1997) in (Sørensen and Sørensen 2010)). No other reference has been found for this system, so it presumably has never been applied, and little information is available.

Load transfer path

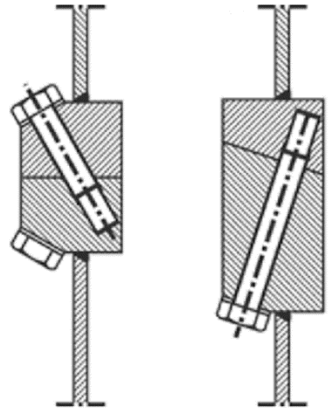

Figure 14 - Eccentric-free bolted joint

The issue of bolts loaded in bending in a conventional bolted connection is avoided in this concept by using bolts diagonally across a thick flange. The loads are transferred through the bolts, but as these cross the centre line, the bolts are loaded both axially and in shear.

Criteria

TRL

No application of this type of connection has been found, nor has any analytical evaluation. It is therefore at TRL 1.

Material

Because of the diagonal bolts, the flanges have to be quite a bit thicker than in a normal bolted flange. Again, no dimensioned drawings are available, so material costs cannot be estimate very accurately. Based on the sketches available, the flanges thickness is circa twice the thickness of conventional bolted flanges.

Item	Quantity	Unit	€/unit	€ x 1000
Forged flange MP/TP	2	-		
M72, grade 10.9 bolts	100	-		
Additional sealing material	-	-		
Total				

Table 6 - Bill of content eccentric-free bolted joint

Manufacturing

The eccentric-free bolted connection requires that the bolts cross the centreline diagonally. This requires a complex drilling operation to ensure the bolt holes in the two flanges line up. Furthermore this hole must be threaded and is blind in the secondary flange, further complicating the machining operation.

Installation

Precise alignment of the flanges is required before the bolts can be inserted. This is complicated by the blind holes in one of the flanges. Similar to conventional bolted designs this concept cannot be applied underwater.

Serviceability

The bolts are directly in the load path, so their tension must be checked regularly. This concept is also sensitive to corrosion, and designing a corrosion protection system is less straightforward as the bolts cross the centreline.

Scalability

This connection has the same issues at very large diameters as conventional bolted connections. These may be further exaggerated by the very thick flanges that are required.

Underwater

It will be very challenging to adapt this connection to be installed underwater.

2.8 Friction connection

Within the framework of the HISTWIN (High-Strength Steel Tower for Wind Turbine) project, a friction connection has been developed as an alternative to bolted flange connections in (onshore) wind turbine towers (Veljkovic et al. 2010).

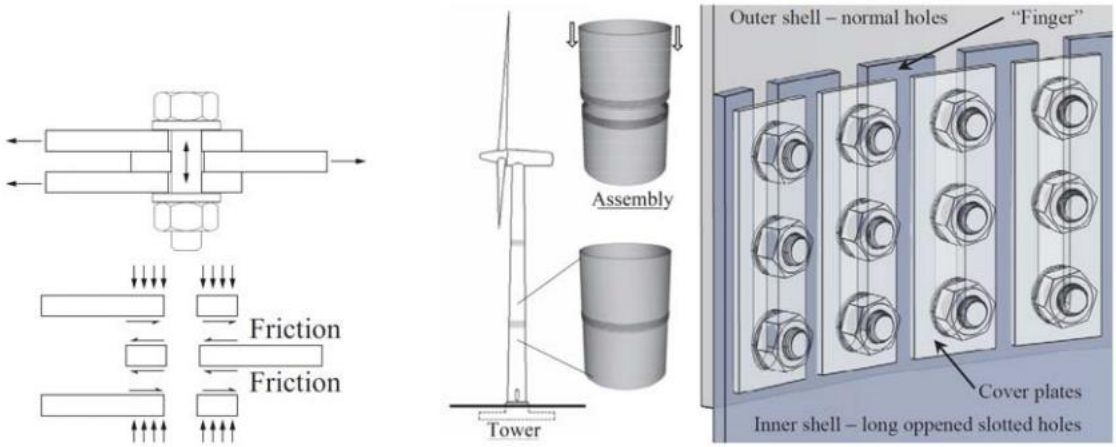

Figure 15 - Load transfer and general arrangement, friction connection

Load transfer path

Loads are transferred between the elements via friction. This friction is provided by clamping force resulting from preloaded horizontal bolts. The bolts are not structurally loaded, they only serve to ensure adequate friction.

TRL

The friction connection has been tested extensively in laboratory setups ((Veljkovic and Husson 2009)) and in FE studies (Pavlović et al. 2015). Therefore a TRL of 4 is probably achieved.

Material

Veljkovic and Husson (2009) performed a cost analysis comparing the friction connection to a bolted flange connection in the application of an onshore wind turbine tower with diameters 3.9 and 3.4 m. The material costs were estimated to be 80% lower than the equivalent flange connection, as no forged flanges are required. Scaling the results from this study to the reference foundation, the following prices are found.

Item	Quantity	Unit	€/unit	€ x 1000
Overlap steel	14.5	t		
Bolts	882	-		
Total				

Manufacturing

The only additional fabrication step required for the friction connection is the cutting of holes in the plates that form the primary steel. This could be done before rolling.

Installation

The friction connection requires around 4 times as many bolts as a flange connection. These bolts are typically smaller and easier to handle, as are the tools to tighten them. This could result in a net advantage compared to flange connections.

Serviceability

Veljkovic et al. (2010) found an estimated loss of pretension of 20% over a lifetime of 20 years. This can be taken into account during the design phase, or by retensioning the bolts. The friction connection is presumably fairly sensitive to corrosion as the connection is reliant

on friction. Furthermore the bolts penetrate the primary steel which complicates sealing the system against corrosion.

Scalability

In comparison with a bolted flange connection, the friction connections appears to be more scalable as the number of bolts per row can be increased.

Underwater

This connection uses a large amount of bolts, which is not feasible underwater.

2.9 Wedge connection

Based on the issues with grout and bolts, a connection using a wedge to connect flanges of large diameter tubulars has been developed at Fistuca. The principles of the wedge connection are introduced in chapter 0. In this section, these principles will be used to analyse the generic wedge connection, similar to analyses performed on the other connection methods.

Criteria

TRL

The technical details of the wedge connection are discussed in chapter 0, and will not be repeated here. At this point, the wedge connection is at TRL 1. This thesis aims to elevate this to TRL 2/3.

Material

The wedge connection requires very little overlapping steel. A basic flange is attached to the top of the monopile, and a more complex flange is fitted to the bottom of the TP. Furthermore a large number of tapered dowels is required. Some of these components are quite unique, so it is difficult to estimate their cost. The bill of content in Table 7 gives a first indication of the material cost of the wedge connection.

Item	Quantity	Unit	€/unit	€ x 1000
MP flange		-		
TP flange		-		
Dowels		-		
Hydraulics		-		
Total				

Table 7 - Bill of content wedge connection

Manufacturing

The MP design can be very straightforward: a hole with a flat, angled surface is machined into a ring. The TP flange geometry is more complex, requiring a cantilevered section with (blind) holes and fittings and hoses for hydraulics. The dowels are rather straightforwardly produced, requiring some machining for the inclined plane.

Installation

Offshore installation of the wedge connection is one of the major advantages. The upper section can be lifted in place without personnel to guide it, as it can be oriented by external guides and/or tapered dowels that are extended first. The only manual work required to fasten the connection is hooking up hydraulics, which can be done onshore. Such an implementation would require no personnel to be present at the connection itself. The wedge

connection cannot correct non-verticality of the upper part by itself. However, it could be feasible to place shims between the lower and the upper part of the connection. A further benefit could be to use a number of dowels for seafastening of the TP to the deck of an installation vessel.

Serviceability

Once installed, the wedge connection requires no specific maintenance. A monitoring system could easily be implemented, as the driving force is hydraulic. Sensors could be included in the cambers to monitor the pressure, which is directly converted into preload of the connection. If a hardening fluid is used, this is of less importance.

The wedge connection is sensitive to corrosion, as it relies on contact. Including protective seals and/or a cathodic protection system is relatively straightforward.

Scalability

The wedge concept seems to be very scalable, as the contact area can be increased in radial direction if stresses become too large. Similarly, both the dowel diameter and number can be increased.

Underwater

The connection can easily be applied underwater. The load-bearing parts are relatively well protected by design, and water ingress could fairly easily be prevented.

2.10 Analysis

To compare the eight different concepts across the seven criteria, Table 8 is used. On some criteria, such as TRL or material cost, a fairly objective assessment can be made in standard units. On other criteria, such as manufacturability and installation, a more subjective approach is required. For these criteria a scale of 1-5 is used, where 1 indicates a poor concept and 5 a great concept. These subjective criteria have been graded after considerable discussion with academic and industry experts. Nevertheless, they remain a subjective measure and should not be considered universal truths. For scalability, the magnitude of scaling material cost with the overall foundation diameter is used. Whether or not the connection concept can be (easily) be applied underwater is indicated by a binary yes/no.

Table 8 - Concept comparison scores

Criterion	TRL	Material	Manufacturing	Installation	Serviceability	Scalability	Underwater
Concept	[-]	[k€]	[-]	[-]	[-]	D^	y/n
Grout	**9**		4	2	3	2	y
Bolt	**9**		3	2	2	1	n
Slip joint	5		3	4	3	2	y?
DSJ	4		2	5	3	2	y
Tension-free	2		3	1	1	1	n
Eccentric-free	1		2	2	1	1	n
Friction	4		5	2	2	2	n
Wedge	1		3	4	4	1	y

2.10.1 Manufacturing cost

Manufacturing costs are difficult to estimate, and have not been quantified. The concepts have been ranked on what kind of metalworking steps are required at what dimensions and tolerances. The **grouted** connection is very simple, but does require grout seals: score of **4**. A **bolted flange** connection requires forged flanges and large size, high strength bolts: **3**. The **slip joint** uses two very large steel components that have to be manufactured precisely, **3.** In the **double slip joint** these conical rings are smaller, but another pair is added: score of **2**. The **tension-free** connection has fairly complex manufacturing requirements (**3**) while the **eccentric-free** concept threaded blind holes are very complex (**2**). The **friction** connection is very simple, requiring only some cuts in the primary steel and potentially a simple cover plate (**5**). The **wedge** connection uses one simple and one complex flange, together with a large number of fairly simple dowels, all in all comparable to a bolted connection: **3**.

2.10.2 Installation

Installation time is one of the main reasons to look beyond the current connection methods. **Grout** takes a very long time to pump, and after that it has to cure: **1**. The need for **bolted** connections to be precisely aligned, and the large number of bolts must be tightened and checked give it a score of **2**. The **slip joint** installation is faster: **4**. In the **double slip joint** concept even this is eliminated: it is installable by self-weight only, **5**. The complex wedge nut of the **tension-free** concept complicates installation (**1**), the other two alternative bolt designs get a score of **2**. Lastly, the **wedge** connection gets a score of **4** as it doesn't need accurate alignment, and is secured via fast hydraulics.

2.10.3 Serviceability

The serviceability of the **grouted** connection is good in that it required no basic service. However if the grout would start to fail, the joint is very hard to repair and susceptible to

corrosion. For these reasons, it gets a score of **3**. The repeated inspection and torqueing of **bolted** joints is very expensive: **1**. The **slip joint** and **double slip joint** both require no specific maintenance, but they are susceptible to corrosion: **3**. The alternative bolt designs share the downsides of the bolted flange design, with an additional deduction for the **eccentric-free** concept for being impossible to inspect. Once the **wedge** connection is installed, it is maintenance-free and it can be protected from corrosion quite well: **4**.

2.11 Advantages and challenges for the wedge connection

The goal of this comparison is to be used as input for the design of the wedge connection. The most important advantages of the wedge concept over the current connection methods are installation, serviceability and the ease of applying the concept at larger diameters and underwater.

Installation can be quicker, safer and cheaper compared to grouting and bolting. The concept allows for a personnel-free installation method. During the design stage, this advantage can be exploited by ensuring the hydraulics are as simple as possible. The upper section shouldn't need exact alignment with the lower section. This results in easier, faster lifting.

The current industry standard of TP-MP connections, bolting, requires frequent inspection and torqueing of the bolts. This can be a large part of O&M costs for an offshore wind farm. If the connection can be designed such that the preload can be guaranteed or at least monitored from distance, a major advantage would be gained compared to bolted connections.

The biggest challenge will be the fabrication of the upper section flange. This is a complicated part, as it must fit within the lower ring, provide a load path and feature radial holes for the dowels and hydraulic lines. The fabrication of the other parts is fairly straightforward.

Another challenging point, especially if the connection is to be applied under water, is corrosion protection.

3 Analysis of the wedge connection

Before an actual design of the wedge connection can be made, some insight into the principles is required. In this section analytical expressions will be derived for the load transfer path. The main principle of the connection is achieving a vertical preload via the inclined plane. The equations governing this relationship are derived in the first section of this chapter. In the next section, friction is introduced.

3.1 Load transfer through preload and dowel

The load path is best illustrated in free body diagrams (FBD) of the unloaded connection. Figure 16 is a simplified FBD of the dowel in its final, stable position. The hydraulic pressure is represented by a horizontal force. The reaction force is provided by a contact force normal to the inclined plane (red arrow). Because of the small wedge angle, this normal force has a large vertical component, which can be expressed as:

$$F_{contact,vert} = \frac{F_{hydraulic}}{\tan(\alpha)} \quad (1)$$

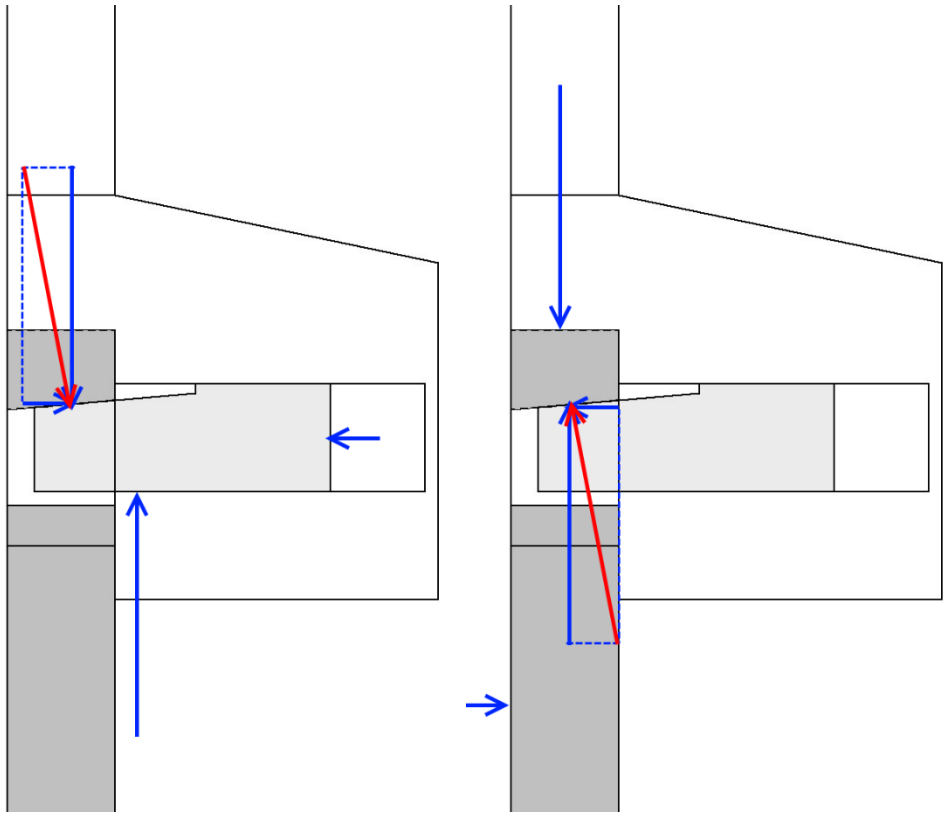

Figure 16 – Left: Free body diagram of the dowel, right: FBD of the MP

Following this contact force, the FBD of the MP flange can be drawn as in Figure 16b. Here a radial force must be provided by the radial stiffness of the pile. The blue arrow at the top of the flange represents the preload P. As indicated in the drawing, the magnitude of this force is:

$$P = F_{contact,vert} = \frac{F_{hydraulic}}{\tan(\alpha)} \quad (2)$$

This equation (2) is the core of the wedge connection.

The load path is closed through the TP. The reaction forces to the preload and to the vertical dowel load cancel each other. The hydraulic pressure has an inward radial component that must be resisted by an outward radial force through the TP flange.

The load path is summarised in Figure 17.

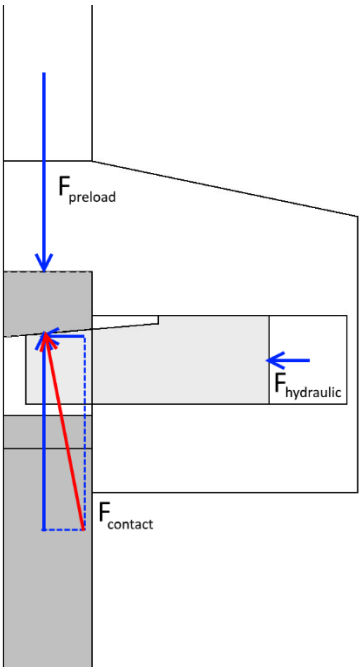

Figure 17 - Load path of the wedge connection

3.1.1 Load sharing between the joint and the dowel

Similar to a bolted flange connection, there are two load transfer mechanisms for tensile load, as long as the flanges remain in compression. One part of the load will be transferred by flanges, another part will be transferred by loading and deforming the dowel. The relationships governing this load sharing are (Integrated Systems Research 2008) based on the :

$$F_{dowel} = P + \frac{k_d}{k_d + k_j} * F_{applied}$$

$$F_{joint} = P - \frac{k_j}{k_d + k_j} * F_{applied}$$

From these equations it follows that if the joint is much stiffer than the dowel ($k_j \gg k_d$), the dowel will take almost none of the external load. Once the applied load is larger than the preload however, the joint will lose compression and open (setting $F_{joint} = 0$ shows this). This

is not desirable, so in practice the joint should be of comparable, but higher, stiffness to the dowel stiffness. In such a situation, the dowel will carry some external load in shear, but the connection is able to transfer a load that is larger than the preload.

Modelling the stiffness of the dowel and the flanges is not straightforward. Due to the relatively thick and short cantilevering section, Euler-Bernoulli beam theory may not be sufficient to describe the dowel behaviour. Instead, Timoshenko beam theory could be more appropriate to include shear deformation.

A further issue complicating an analytical solution is the boundary condition at the clamped end of the dowel. The dowel is held in place only by contact with the dowel hole in the TP. This is an elastic boundary, with uncertain stiffness and length.

The same holds for the stiffness of the flanges. The area around the dowel is loaded similar to the end of a plate in a bolted lap joint, but a key unknown is what thickness can be taken into account in determining the stress field. An analytical approach is feasible, but must be verified carefully. Brown et al. (2008) present a good overview of analytical methods in use for bolted flange design. Similar techniques of estimating the area of the stress field in the flanges could be applied for the wedge connection.

A more practical approach to determine the load distribution is to use FE modelling. A first attempt to do so can be found in section 5.2.3.

3.2 Contact surfaces and friction

3.2.1 Friction coefficient

As the wedge connection relies on contact between surfaces with large normal loads, friction will be an important factor. In an analytical model like considered in this section, contact is defined by transfer of loads normal to the surfaces in contact. This is always accompanied by friction parallel to the surface in reality. The nature of friction is not fully understood, and many models exist to explain the phenomenon. The classical theory of friction has been developed by Amontons (1699) and Coulomb (1781) (in (Nolle and Richardson 1974)), stating that:

- The force of friction is directly proportional to the applied load.
- The force of friction is independent of the apparent area of contact.
- Kinetic friction is independent of the sliding velocity.

Or simply in the expression

$$F_{fr} \leq \mu * N$$

This Coulomb model of friction is based on empirical data, and values for μ are presented in tables for different interacting materials. Often a distinction is made between 'static' and 'kinetic friction coefficients. The values found in literature often don't agree with each other, and the fundamental origins of friction have not been fully captured in a theoretical framework. Many attempts to do so result in models that take into account additional factors such as contact area and/or pressure. Nevertheless, the Coulomb friction model remains the most practically appropriate friction model for engineering purposes, under the condition that the friction coefficient is determined from a test appropriate for the purpose.

Many factors influence frictional behaviour. Therefore the coefficient μ to be used in a situation must be measured under similar circumstances (Blau 2001). Nolle and Richardson (1974) presented a review on experimental data on static friction between steel surfaces.

Most data was obtained using point-contact devices, such as (half-)spheres sliding on planes, in which the contact pressure is not constant over the contact area. There was also no standard method of preparing and cleaning the surfaces. A large range of static friction coefficients was found, ranging from 0.3 to 1.0.

The value of the friction coefficient must be selected from a test similar to the application, in this case, flat-on-flat, static steel contact (Blau 2001). Nolle and Richardson (1974) performed such tests, using different contact pressures (0.68 to 68 MPa) and surface finishes. For machined (turned or ground) surfaces, a static friction coefficient of 0.19 was found, regardless of contact pressure. The surface roughness (*Ra)* in these tests was circa 1.5 μm. A closer finish ($Ra < 1\ \mu m$), still achievable with common machining operations, leads to a friction coefficient of ca. μ=0.1.

For an even lower friction coefficient of 0.05, a surface roughness of circa 0.2 μm is required. This can be achieved by lapping or honing the surface. Alternatively (or additionally), the interface can be lubricated to reduce friction.

3.2.2 Lubrication of the contact surfaces

The friction along the contact surfaces can be reduced by lubrication. This can either take the form of fluid lubrication (e.g. grease) or solid lubrication (e.g. PTFE, graphite or molybdenum disulphide). There is little data to be found on friction coefficients for lubricating agents, as these are quite dependent on the configuration of the friction system. Nevertheless, some generic review studies provide an indication. These are summarised in the table below.

Lubricating mechanism	**Type**	**Typical μ**	**Notes**	**Reference**
Hydrodynamic	Fluid	0.01	Load is fully taken by the fluid. $h_{fluid} \gg R_a$. Low load bearing capacity	(Holmberg and Matthews 2009)
Elasto-hydrodynamic	Fluid	0.05	Very thin fluid layer, with some load transfer through bodies. $h_{fluid} \approx R_a$	”
Boundary:	Fluid	0.1	Load transfer between bodies, thin film of lubricant adsorbs to the solid and reduces shear strength. No hydrodynamics. $h_{fluid} \to 0$	”
PTFE	Solid	0.02 – 0.1	Relatively low load bearing capacity	(Miyoshi 2007)
Graphite	Solid	0.07 – 0.5	Relies on adsorbed moisture, promotes electrolysis (corrosion)	(Kopeliovic 2012)
MoS_2	Solid	0.03 - 0.1	Sensitive to humidity	(Winer 1967)

The optimal system will have to be found experimentally for this specific application.

3.2.3 Friction in the wedge connection

The FBD’s presented in section 3.1 are redrawn here to include friction. Equilibrium equations are also included.

The dowel experiences friction along the bore and along the inclined plane, see the FBD in Figure 18. The equilibrium equations are as follows:

$$\sum F_x = F_{TP,fr} + F_{MP,fr} * \cos(\alpha) + F_{MP,N} * \sin(\alpha) - F_{hydr} = 0$$

$$\sum F_y = F_{TP,N} + F_{MP,fr} * \sin(\alpha) - F_{MP,N} * \cos(\alpha) = 0$$

(3)

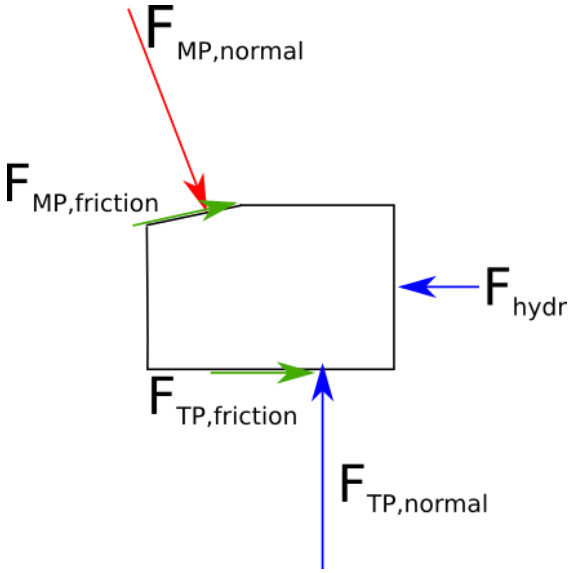

Figure 18 - FBD of the dowel, including friction

The key unknown is the friction along the dowel and TP, $F_{TP,fr}$. If this term of the equation is set to zero, an analytical solution can be found with the assumption that the full frictional capacity along the wedge area is used. This leads to eq. (4).

$$F_{MP,N} = \frac{F_{hydr}}{\left(\sin(\alpha) + \mu_{wedge} * \cos(\alpha)\right)}$$

(4)

Additionally, $F_{pre} = F_{MP,N} * \cos(\alpha)$ and thus

$$F_{pre} = \frac{F_{hydr} * \cos(\alpha)}{\left(\sin(\alpha) + \mu_{wedge} * \cos(\alpha)\right)}$$

This relationship is used in the next section to select the wedge angle of the preliminary design.

4 Preliminary design

A preliminary design is required as input for a more detailed analysis. The geometry and dimensions of this design are calculated using basic analytical equations, based on conservative assumptions regarding the load sharing between joint and dowel. The wedge connection is designed for a monopile foundation of 10 m, where the connection is made below the waterline. Additionally a design is produced for a 6 m diameter monopile to allow direct comparison to bolted connection which exist at this scale. The goal of this parallel development is directly compare the wedge connection to a bolted connection, and to explore the advantages of the wedge connection at a larger diameter.

4.1 Design goals and method: self-locking and allowable stress

The goal of this phase is to develop an initial design to be used as input for later iterations, based on the physical principles of the wedge connection. The most critical design requirement is that the connection must fulfil its load transfer function at all loads encountered during the structure's life. In practical terms for the initial design this means that at ULS loads, no global yielding may occur. The exact distribution of loads over the dowel and the joint is dependent on the relative stiffness of these components. The stiffness is a result of the design, and how each component interacts is unknown at this point. Therefore conservative assumptions must be made at this stage.

The initial dimensioning is based on the shear strength of the dowel, and the contact pressure over the inclined plane. Both are designed to transfer the full ULS tensile load. Additionally it is required that the wedge is self-locking, meaning that it does not slide out of the connection even if the horizontal hydraulic pressure is removed.

4.2 Design loads and requirements: reference cases and Hybrid Monopile

The wedge connection must be able to transfer all loads from the turbine to the foundation. The loads are governed by environmental conditions and structural geometry. The preliminary design is based on ULS. The loads at the connection level have been calculated as part of the Hybrid Monopile project. The wedge connection will be designed for two structures: a conventional MP and a new Fistuca design, the hybrid monopile. The conventional MP will be used as a reference case and comparison to the bolted flange connection, as in chapter 2. Some properties of these structures can be found in Table 9.

4.2.1 Defining design variables

The core of the wedge connection is the inclined plane between the dowel and the MP flange. The following design variables are key to the inclined plane and thus the wedge connection:

- Wedge angle
- Contact surface area between dowel and MP
- Number of dowels / centre-to-centre distance dowels

These variables will drive further design of the wedge connection.

Table 9 - Structural details of conventional and hybrid monopiles

Property	**Unit**	**Conventional connection**	**Underwater connection**	**Underwater connection Hybrid**
Turbine site	-	North Sea	North Sea	North Sea
Turbine rated power	MW			
Water depth	m - LAT			
Connection diameter	m			
Connection level	M - LAT			
Wall thickness TP at connection	mm			
Design axial load at connection	MN			
Design bending moment at connection	MNm			
Design tensile stress at connection	N/mm²			
Design compressive stress at connection	N/mm²			

4.3 Setting the wedge angle

To achieve a self-locking wedge, the wedge angle must be small enough that the wedge does not leave the connection under an applied vertical load, even if the hydraulic pressure would drop out. The FBD of the dowel in this situation is given in Figure 18.

The equilibrium equations are:

$$\sum F_y = F_{TP,N} - F_{MP,N} * \cos(\alpha) - F_{MP,fr} * \sin(\alpha) = 0$$

$$\sum F_x = F_{MP,N} * \sin(\alpha) - F_{MP,fr} * \cos(\alpha) - F_{TP,fr} = 0$$

Considering the wedge is on the verge of sliding:

$$F_{fr} = \mu_{wedge} * F_N$$

Substituting this into the equilibrium equations:

$$F_{TP,N} - F_{MP,N} * \cos(\alpha) - F_{MP,N} * \mu_{wedge} * \sin(\alpha) = 0$$

$$F_{MP,N} * \sin(\alpha) - F_{MP,N} * \mu_{wedge} * \cos(\alpha) - F_{TP,N} * \mu = 0$$

From this we find

$$F_{TP,N} = F_{MP,N} * \big(\cos(\alpha) + \mu_{wedge} * \sin(\alpha)\big)$$

Which can be substituted to find

$$F_{MP,N} * \big(\sin(\alpha) - \mu_{wedge} * \cos(\alpha)\big) = \mathrm{F}_{MP,N} * \big(\cos(\alpha) + \mu_{wedge} * \sin(\alpha)\big) * \mu$$

Taking out $F_{MP,N}$ and rearranging, we find

$$\sin(\alpha) - \mu_{wedge} \cos(\alpha) = \mu_{\mathrm{wedge}}(\cos(\alpha) + \mu \sin(\alpha))$$

Which can be rearranged to find

$$\alpha = \text{atan}\left(\frac{2\mu_{wedge}}{1+\mu_{wedge}^2}\right) \tag{5}$$

Plotting the results of eq. (5) for various friction coefficients, Figure 19 is obtained. To select a safe, conservative wedge angle, a small friction coefficient has to be selected. In (Nolle and Richardson 1974), a static friction coefficient of 0.19 was found in flat-on-flat contact between machined surfaces for a range of contact pressures. This is a lower value than is typically quoted in engineering tables (such as 0.75 in (Ramsdale n.d.)), but similar to the friction coefficient of 0.2, specified in offshore steel structure standards (DNV GL 2015) for untreated steel surfaces. Using a (very) conservative friction coefficient of 0.1 results in a upper bound to the wedge angle of 11°. Any angle lower than this will ensure self-locking of the wedge.

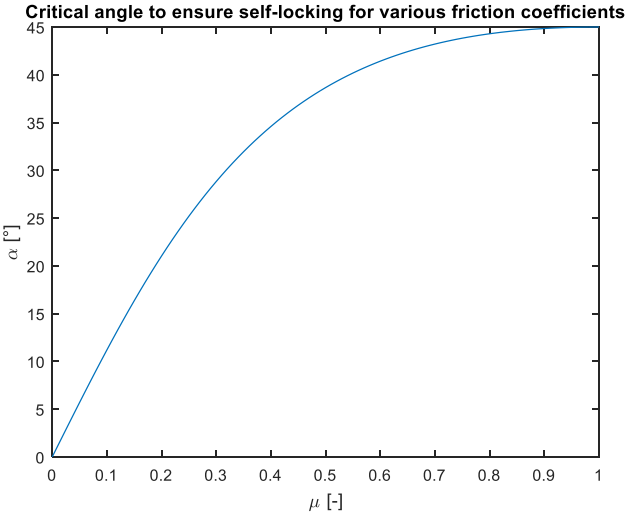

Figure 19 - Critical wedge angle to ensure self-locking

The principle of the wedge connection is the inclined plane. The mechanical advantage of the inclined plane in this situation can be described as:

$$MA = \frac{F_{pre}}{F_{hydr}}$$

The hydraulic force required ensure the required preload can be derived from the equilibrium equations (Section 0). Under the assumption of zero friction along the dowel hole, and full realisation of friction along the wedge area, the relation of eq. (6) was found.

$$F_{MP,N} = \frac{F_{hydr}}{\left(\sin(\alpha) + \mu_{wedge} * \cos(\alpha)\right)} \tag{6}]$$

This can be rearranged into a mechanical advantage relation:

$$MA = \frac{F_{MP,N}}{F_{hydr}} = \frac{1}{\sin(\alpha) + \mu_{wedge} * \cos(\alpha)}$$

Plotting this relationship for angles from 0.5 to 11 degrees, and for various friction coefficients, Figure 20 is obtained. Here it is clear that the wedge angle has a large influence on the mechanical advantage, for all friction coefficients. The smaller the dowel angle, the more advantageous the connection can be made from a force perspective. However there is a practical limit to how small a surface can be accurately machined, especially considering the large diameter involved. For the preliminary design, a wedge angle of 5 degrees is selected. It must be noted that the relationship used here is excluding friction along the dowel. Only friction at the inclined plane is considered.

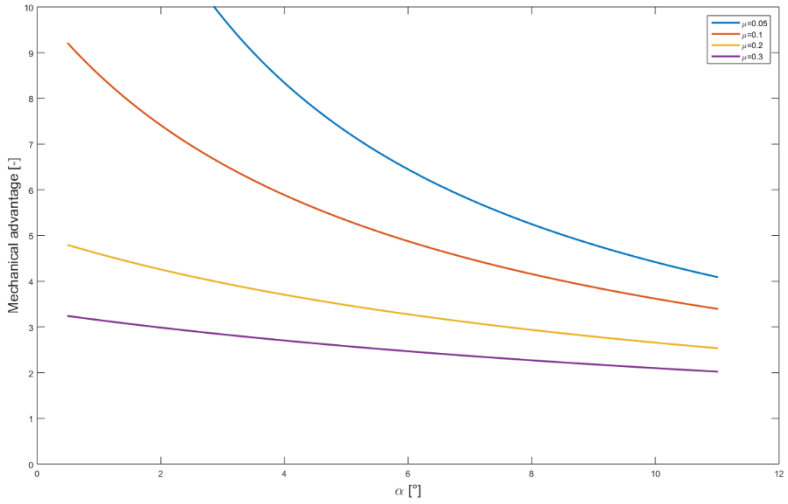

Figure 20 - Mechanical advantage of wedge for small wedge angles, and various friction coefficients

4.4 Dowel number and geometry

4.4.1 Dowel geometry: cylindrical dowel

The dowel is cylindrical with a inclined plane at the end. The expected governing load case for the dowel is the shear across the transition from TP to MP. If there is zero preload, the full ULS tensile load is transferred through this plane. This is a very conservative assumption, as a significant part of the load will be carried by the preloaded flanges.

The number of dowels in the connection is determined from three parameters, using the relationship

$$N_{dow} = \frac{\pi * D_{tp}}{k * D_{dow}}$$

Where k is the centre-to-centre spacing in terms of dowel diameter.

The shear area is calculated from the dowel radius and the point where the contact area is formed, see Figure 21.

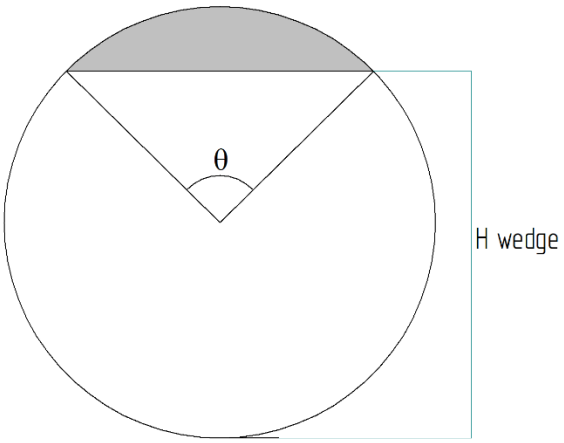

Figure 21 - Definition of shear area in the dowel

$$\theta = 2 * \arccos\left(\frac{h_{wedge}}{R}\right)$$

$$A_{shear} = \pi * R^2 - \left(\left(\frac{R^2}{2}\right) * \left(\frac{\theta * \pi}{180} - \sin(\theta)\right)\right)$$

The width of the contact area is given as

$$chord = 2 * R * \sin\left(\frac{\theta}{2}\right)$$

From the previously calculated total required contact area, the length of the contact area can be found using

$$l_{contact} = \frac{A_{contact\ total}}{N_{dow} * chord}$$

The largest stress in the dowel is assumed to be due to the shear loading, as the dowel transfers the largest tensile load on the connection through shear. The bending moment is neglected, as the arm of the applied load is relatively short. Additionally, the highest stresses in the cross section due to bending moment are found at the top and bottom of the section, while the shear load is transferred mainly through the centre.

This stress can be found by considering a slice of the dowel section (Figure 21). The shear stress on such a slice is given with:

$$\sigma_{xm} = -\frac{V_z S_z}{b I_{zz}}$$

Where V_z is the shear load, S_z is the first moment of area of the slice, b the width of the slice, and I_{zz} the second area moment of inertia of the entire area of the dowel.

$$S_z = \frac{2}{3} * R * \sin(\phi)^3$$

$$b = 2 * R * \sin(\phi)$$

$$I_{zz} = \frac{1}{4}R^4 \int_{-\theta}^{\frac{\pi}{2}} (1 - \cos(4\phi))d\phi$$

This results in a shear stress profile as in Figure 22, with a maximum at the centre of the dowel.

[removed]

Figure 22 - Shear stress profile in dowel

The largest allowable shear stress can be calculated using the Von Mises yield criterion, suggesting $\tau_{allow} = \frac{1}{\sqrt{3}}\sigma_{yield}$.
This procedure is followed for a range of dowel diameters and the fraction of the height at which the inclined plane is placed. The dowel that returns the lowest total volume while still passing the shear stress check is used as initial design.

4.4.2 Dowel length to enable contact and provide adequate clamping

The length of the dowel still inside the TP flange must be sufficient to provide a fixed connection for the cantilever section of the dowel. For conventional fixed dowel pins in mechanical engineering design the engagement length is 1.5 to $2 * D$ (Henriksen 1973). Given the relatively short cantilevering section, $2*D$ is used for the preliminary design.

4.4.3 Resulting dowel geometry

The following geometry is found for the three cases. The length of the inclined plane found in 4.4.1 is quite short compared to the MP flange thickness. To facilitate the load transfer, the inclined plane length is increased to 75% of the MP flange thickness for both 10 m foundations. In these cases, the original, minimally required length is indicated in brackets.

Table 10 - Dowel dimensions

Parameter	**6 m reference**	**10 m monopile**	**10 m Hybrid Monopile**
Number of dowels			
Diameter of dowels [mm]			
H_Wedge [-]			
Length of inclined plane [mm]			
Engagement length [mm]			
Total dowel length [mm]			

4.4.4 Check of bending stress assumption

With the design of the dowel, the assumption that the bending moment in the dowel is negligible can be verified. The governing cross section is assumed to be at the start of the cantilevering section (Figure 21). The bending moment to be transferred:

$$M_z = \sigma_{contact} * A_{contact} * \frac{1}{2} * l_{contact}$$

With

$$\sigma_z^M = \frac{M_z * Izz}{z}$$

This stress due to bending can be combined with the shear stress σ_{xm} from the previous section using the Von Mises equivalent stress:

$$\sigma_{Von\ Mises} = \sqrt{\sigma_z^2 + 3\sigma_{xm}^2}$$

The shear, bending and Von Mises equivalent stress are plotted in Figure 23, with the left side cross section to demonstrate the stress distribution. Including the bending stress does not change the governing Von Mises stress level, which is still at the centre of the dowel. Therefore the assumption that the bending stress can be excluded from the design calculation is valid.

[removed]

Figure 23 - Stress distribution over dowel cross section

4.5 Flange geometry

4.5.1 Primary steel thickness

For the initial design of the wedge connection, it is assumed the primary, vertical steel of the both the MP and TP is identical to that of the reference designs. The wall thickness is 79 mm for both the MP and the TP primary steel of the 6 m foundation.

The 10 m monopile foundation has a 80 mm wall thickness at the connection level. In the Hybrid Monopile, wall thickness is reduced to 53 mm. This is possible due to the increase in diameter and (relative) decrease of loads caused by the braced section.

4.5.2 MP flange design

Only the inclined plane of the dowel should come into contact with the MP. Therefore a generously sized rectangular hole with a width equal to the dowel diameter plus 10 mm is assumed. The height of this hole is assumed to be equal to the height of the remaining section of the dowel plus 10 mm. The height of the flange is set at 2 times the dowel diameter, and the dowel is placed at its centre. Below this flange, a transitional section of 150 mm tall tapers to the primary steel thickness. The dimensions of the MP flange for various geometries are given below.

Table 11 - MP flange dimensions

Parameter	6 m reference	10 m monopile	10 m Hybrid Monopile
Height of flange			
Thickness flange			
Height hole			
Width hole			

[removed]

Figure 24 - MP dimensions for 10 m connection

4.5.3 TP flange design

The TP flange is considerably more complex than the MP flange, as it contains the dowels. The dowel dimensions therefore drive the design of this flange. For the preliminary design it is assumed that the dowels have an exact fit in their holes, so the hole dimensions are equal to the dowel dimensions. A chamber of 10 mm is added behind the dowel for hydraulics, and behind that the wall thickness is also set at 10 mm.

The flange height below the dowel hole is similar to the end distance as found in bolted connections. The minimum end distance in this application is 1.5*D. This guideline is followed for the initial design of the wedge connection.

Above the TP-MP interface, a vertical section of 50 mm is incorporated to provide additional stiffness before a 50 mm tall tapered section towards the narrower primary steel.

For the Hybrid Monopile, the cylindrical braces are fitted to the top of the flange. This complex connection is the subject of a separate study. For the preliminary design, it is assumed that the braces are connected to the full width of the flange, so no tapered section is included.

Table 12 - TP flange dimensions

Parameter	**6 m reference**	**10 m monopile**	**10 m Hybrid Monopile**
Diameter hole			
Depth hole			
Height of lower part of flange			
Thickness lower flange			
Thickness MP/TP interface			
Thickness middle part of flange			

[removed]

Figure 25 - TP dimensions for 10 m connection

4.6 Preliminary design

The main preliminary dimensions of the wedge connection for the 10 m base case are presented in Figure 26.

[removed]

Figure 26 - Preliminary dimensions wedge connection for 10 m foundation

5 STRUCTURAL ANALYSIS

To analyse the complex geometry and load path of the wedge connection, two finite element models are created using ANSYS. The first model allows studying the behaviour of connection as a whole under loads. The second model is used for a more detailed analysis of the dowel. First the techniques used to model the connection are described. The more general model is used to generate load-displacement curves which are used to analyse the behaviour and stiffness of the structure. Various parameters that might affect the performance of the connection are investigated. The second model is used to analyse stresses and plasticity effects in the dowel.

5.1 Modelling the wedge connection in ANSYS

The finite element method is used to find a numerical solution to the problem of interacting, deformable bodies that is the essence of the wedge connection. The software package ANSYS Mechanical APDL is used. This system offers many different element types, allows for parametric geometry design and has various options for simulating contact surfaces.

5.1.1 Implicit, static analysis

The goal of the wedge connection is to rigidly fix two large diameter tubulars together. A dynamic analysis of the connection is therefore not required. Static analysis will be used to check deformations and stresses in the connection. Typically implicit calculation schemes are stable and more efficient for static problems, as they can use larger time steps compared to explicit schemes. Therefore an implicit finite element analysis will be used.

The wedge connection problem is mostly linear, except for the contact surfaces. Implicit schemes require a number of iterations to reach equilibrium within each time step in non-linear problems.

The Newton-Raphson Procedure is used to solve the non-linear equations. To demonstrate numerical convergence, the h-method is applied. In this method the element size h is decreased to find a new solution to the problem. If this solution is sufficiently similar to the original solution, the problem is considered to be converged.

5.1.2 Geometry: Cyclic symmetry

The wedge connection is a cyclic symmetrical system. ANSYS can perform automatic analysis of cyclic symmetrical structures by adding appropriate boundary conditions during solving. The full structure can be visualised in post-processing, if required. The finite element analysis can thus be performed on just a single, 'basic' sector. Three volumes are defined: TP flange, MP flange and the dowel. The geometry of the 10 m diameter foundations with the connection below the waterline is used. For comparison to a bolted connection at 6 m diameter, a model has also been developed for the 6 m geometry.

A section of primary steel is included in the model on both the MP and TP side (Figure 27). The dowel is fitted into its hole in the TP flange, and is positioned at partial stroke to ensure contact between the inclined planes from the beginning of the simulation.

[removed]

Figure 27 –Left: General arrangement. Right: single sector, with MP flange in orange, dowel in red, TP flange in blue.

5.1.3 Solid elements and meshing

The basic sector is meshed using the SOLID187 element type. This is a higher-order solid element that displays quadratic displacement behaviour. It uses 10 nodes per tetrahedral element. It is especially suitable for simulating irregular geometry, such as the small taper angles and the cylindrical shape of the dowel (Wang, Nelson, and Rauch n.d.).

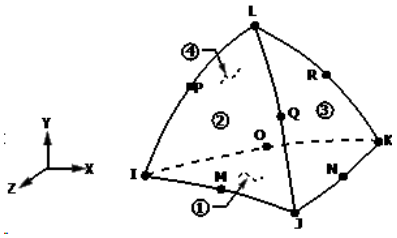

Figure 28 - Geometry of tetrahedral SOLID187 element

A free mesh is used to allow the tetrahedral elements to wrap around the curvature of the solid structure. The SmartSizing algorithm is used to determine element sizes. This algorithm computes estimated edge lengths for all lines in the volumes to be meshed. These are refined for curvature, and connecting lines are drawn to form the actual elements.

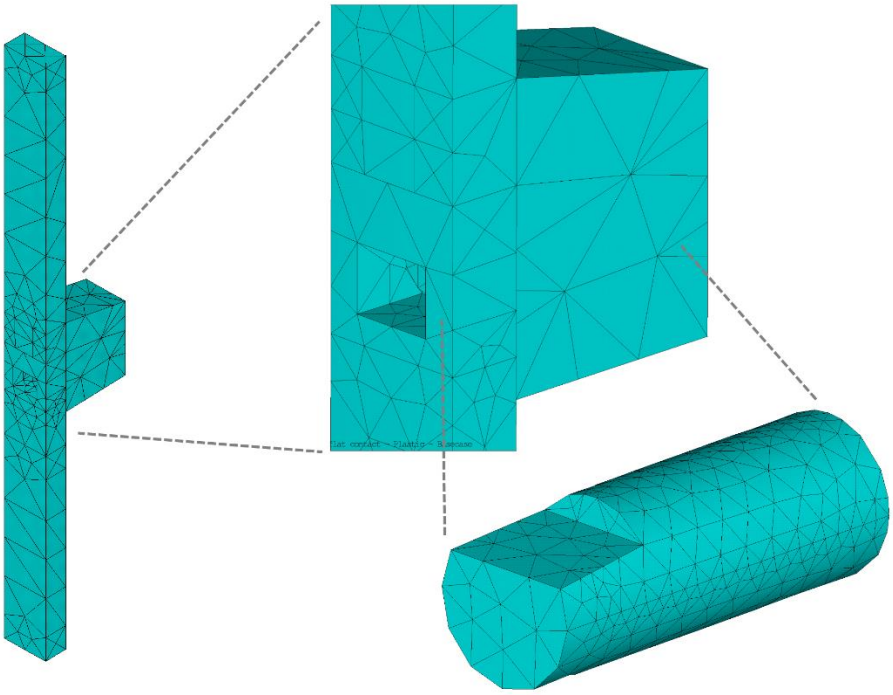

Figure 29 - Default mesh, density = 6

5.1.4 Contact surfaces

Because it is clear which parts of the system are in contact with each other, pair-based contact is selected. In this technique contact is simulated between pre-specified contact elements and target elements. The various contact areas are indicated with different colours in Figure 30.

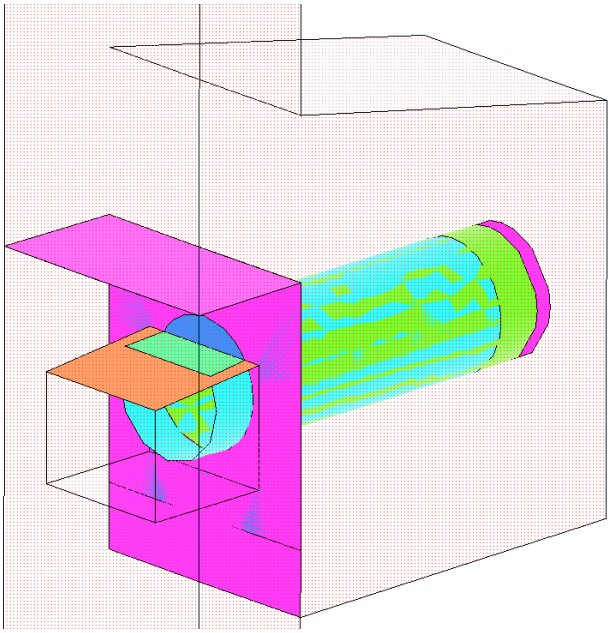

Figure 30 - Contact pairs

ANSYS uses the element type TARGE170 for 3-D targets. For the contact surfaces, several different element types are available. CONTA174 is used in this problem, as this is a 3-D higher order element, matching with the SOLID187 element type used for the solid bodies.

The target and contact elements are 'pasted' to the mesh of the solid model. This ensures that the elements align and loads are transferred correctly from the contacting surfaces to the solid model underneath.

Several contact algorithms are available in ANSYS. The augmented Lagrange method is selected for this problem. In this method, the normal force transferred between elements is found as:

$$F_{normal} = k_{normal} * x_{penetration} + \lambda$$

This is a penalty-based method. The contacting surfaces are allowed to penetrate somewhat. Choosing a very large value for contact stiffness k_{normal} would lead to very small penetration, but this is numerically unstable as the surfaces may bounce off each other. Therefore the augmented Lagrange method adopts an extra term λ, making the method less sensitive to contact stiffness.

To speed up simulation, a so-called Pinball Region is defined around each contact detection point to differentiate between near and far open contact. If a target node is within the pinball sphere, the point will be monitored closely by the programme to determine if contact is established. This state is considered 'near open' contact. If no target node is found within the pinball sphere, the contact status is 'far open' contact.

5.1.5 Friction model

A basic Coulomb friction model is implemented for elements that are in contact. The contacting surfaces can transfer shear stresses up to $\tau_{max} = \mu * p$. The surfaces will slide relative to each other if this shear stress is exceeded. The contact status in that case is 'sliding'. Otherwise, the contact status is 'sticking'.

5.1.6 Boundary conditions and loading procedure

A fixed boundary condition is applied to the bottom of the MP flange, to prevent free movement of the solid bodies. The dowel and TP flange are only constrained by the contact areas. ANSYS automatically generates appropriate boundary conditions constraining the sides of the basic sector, to simulate the full ring stiffness, and applies all defined loads to each sector.

Two loads steps are defined: first the pressure is applied to back of the dowel, pushing it into its installed position. This pressure is deleted in the second load step, and a displacement load is applied to the top of the TP section. Both loads are gradually increased during the load steps. The maximum displacement is selected such that it results in a stress greater than ULS load in the primary steel.

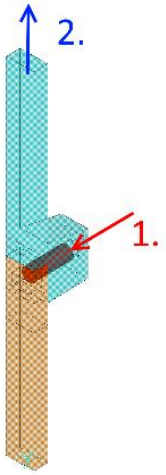

Figure 31 - Loads on the structure

5.1.7 Analysing the results

To study the behaviour of the wedge connection under loads, load-displacement curves are be used. A positive (tensile) displacement load is incrementally applied to the top of TP section. The vertical reaction force at the fixed boundary condition at the bottom of the MP section is measured, and the mean stress is calculated to compare with the ULS stress.

[removed]

Figure 32 - Typical contact status during tensile loading

5.2 Base case results

The base case has been defined with the geometry of the 10 m, underwater connection from section 0. The friction coefficient value is initially set at 0.05, which is a low, but realistic value for machined and lubricated steel surfaces (see section 3.2). The input pressure on the back of the dowel is set at [removed] bar, and the yield point of the material model is taken as 355 N/mm².

[removed]

Figure 33 - Stress - gap plot base case

Figure 33 shows a plot of the stress in the primary steel of the structure versus the maximum and minimum gap in the MP-TP interface. A horizontal line is drawn at the largest tensile stress.

5.2.1 Validation of model and comparison to analytical calculation

To validate the physics of the model, a comparison to analytical calculations can be made. Using the relation between hydraulic force and preload on the connection (eq. (4 from section 3.2.3, repeated in (7)), a comparison can be made between the numerical and analytical models.

$$F_{MP,N} = \frac{F_{hydr}}{(\sin(\alpha) + \mu * \cos(\alpha))} \qquad (7)$$

5.2.2 Preload development

One of the components of the load transfer path of the wedge connection is a preload between the MP and TP flanges. The development during the first load step, and the subsequent loss of preload during the second load step is plotted in Figure 34. As the self-weight of the structure is not taken into account during the first load step, the preload starts at zero. During the second load step, the self-weight is incorporated as a negative normal load, reducing the applied tensile stress.

[removed]

Figure 34 - Development of preload during first and second load step

5.2.3 Load sharing between the dowel and flanges

To investigate the load sharing between the dowel and flanges, the shear in the dowel and the contact force in the MP/TP interface are extracted from the FE model. Figure 35 indicates, as expected, a loss of preload and an increase in shear in the dowel as the tensile load increases. This indicates that both mechanisms take some fraction of the load. To closer investigate the ratio between these mechanisms, the following fractions have been introduced, representing the gain in shear and loss of preload relative to the applied load. The changing fractions of load transfer are plotted in Figure 36.

$$f_{V_{dow}} = \frac{V - V_1}{F_{applied}}$$

$$f_{preload} = \frac{P_1 - P}{F_{applied}}$$

With V_1 and P_1 the initial dowel shear and preload.

[removed]

Figure 35 - Load sharing between the dowel and flanges in base case FE model

[removed]

Figure 36 - Distribution of load transfer between dowel and flanges

5.3 Parameter study

To study the sensitivity of the concept to a number parameters and gain understanding in factors driving the design, a study has been performed where the base case design is changed slightly.

5.3.1 Dowel pressure

[removed]

Figure 37 – Stress – gap plot for different dowel pressures

[removed]

Figure 38 - The influence of input pressure on the stress at which the connection opens

The stress-gap plot in Figure 37, and the bar plot in Figure 38 show the expected pattern of higher pressures providing more stiffness.

5.3.2 Friction

[removed]

Figure 39 - Stress - gap plot for different friction coefficients

Friction along the contact surfaces plays a crucial role in the wedge connection, as seen in Figure 39.

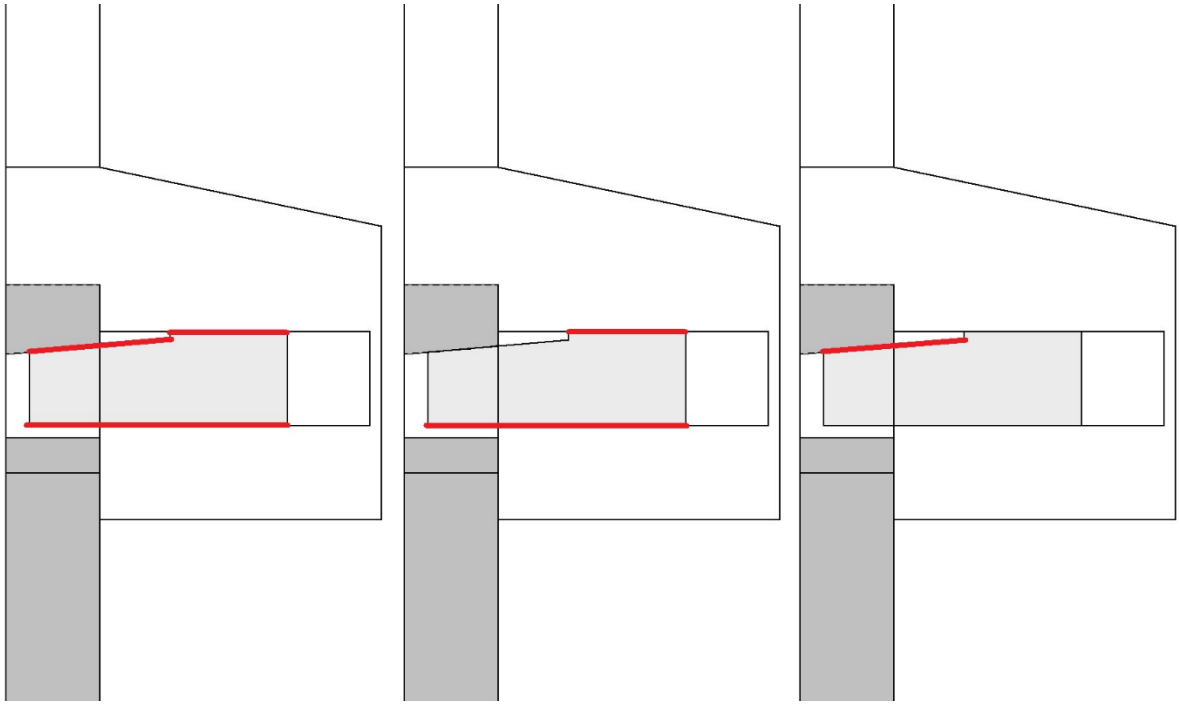

Figure 40 - From left to right: All frictional surfaces, cylinder, inclined plane

[removed]

Figure 41 - The influence of various friction coefficients on the stress at which the connection opens

5.3.3 Yield strength

[removed]

Figure 42 – Opening stresses for different steel grades

Another property that could be of interest for improving the structure's behaviour is the material yield point.

5.3.4 Wedge angle

From the initial analytical calculations the wedge angle came forward as the most critical geometrical parameter (Section 4.3).

[removed]

Figure 43 - Stress-gap plot for different wedge angles

5.3.5 Mesh size

[removed]

Figure 44 - Stress - gap plot for different mesh sizes

One way to study the accuracy of the numerical solution is to perform a study into finer mesh sizes. The default mesh size used in the ANSYS model is 6, leading to ~14000 elements. The results of using a mesh of size 4, 5, 6 and 7 are plotted in Figure 44. These models have between ~2000 and ~30000 elements. At stresses below ULS, there are only very minor differences between the solutions, except for the very crude mesh with size 7. Therefore the model with mesh size 6 is believed to be accurate in terms of element size.

5.3.6 Boundary conditions

[removed]

Figure 45 - Stress - gap plot for different boundary conditions (the red line of the default case is hidden behind the green line of the free rotation case)

Another property of the numerical model that might influence the results are the boundary conditions. The default model uses cyclic symmetry boundary conditions at the sides of the MP and TP, and a fixed displacement and rotation boundary condition at the bottom of the MP. Figure 45 plots results for variations of the model where these two boundary conditions are removed

5.3.7 Reversed and repeated loading

[removed]

Figure 46 - Plastic strain in the TP after the first tensile load step

[removed]

Figure 47 - Stress-gap plot for consecutive load steps

5.3.8 Comparison to bolted flange connection 6 m diameter

No detailed reference design for a bolted connection at 10 m diameter is available, as no foundations of this size have yet been applied. Therefore, a design for a 6 m diameter bolted connection was used to compare with the Wedge Connection

To find the load-displacement behaviour of the reference bolted connection, it was also modelled in ANSYS. To simulate the preload in the bolts, the PRETS179 element type was used. The bolt and washers are modelled as cylindrical bodies, so no threads are modelled. This follows the guidelines set by Kim, Yoon, and Kang (2007) for bolt modelling. The solution was found and post-processed using the same procedure as the wedge connection.

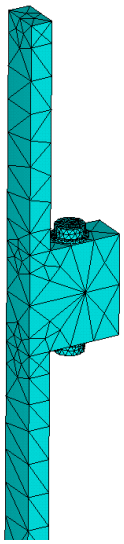

Figure 48 - The bolted flange ANSYS model

[removed]

Figure 49 - Stress-gap plot for bolted flange and wedge connection

The result, plotted in Figure 49.

5.4 Sensitivity to tolerances

Because the Wedge Connection relies on contact surfaces, the fabrication tolerances of the various parts must be investigated closely. Three parts are identified as critical in terms of fabrication and installation: the dowel hole, the inclined plane and the rotational alignment of the TP and dowels with respect to the MP.

5.4.1 Dowel hole

The largest contact surface is the cylindrical hole where the dowel fits in the TP. Initially the diameter of this hole and the dowel is assumed to be equal. To investigate tolerances, the diameter of the hole has been increased slightly with 0.1, 0.25 and 1 mm. Figure 52 shows a sketch of these different diameters.

[removed]

Figure 50 - Sketch indicating the gap between dowel and dowel hole in TP

The results are plotted in Figure 51.

[removed]

Figure 51 – First and full opening stresses for difference between dowel and hole diameter

5.4.2 Inclined plane angle

The second important contact surface is the inclined plane of the dowel and MP hole. Initially, these are set exactly equal at 5°. A discrepancy between these two angles will lead to a smaller contact area and/or more deformation in the cantilever section of the dowel (Figure 52). The effect of such a mismatch is plotted in Figure 53.

[removed]

Figure 52 - Sketch of non-equal dowel and MP hole angles

[removed]

Figure 53 – First and full opening stresses for non-equal dowel and MP hole angles

5.4.3 TP rotational alignment

During the installation process, the TP is lifted onto the MP

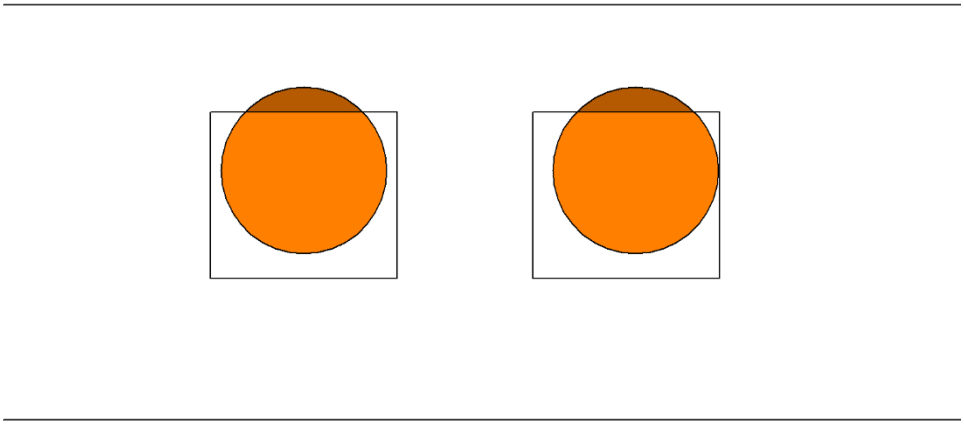

Figure 54 - Left: dowel in MP hole as designed; right: dowel in MP hole with 5 mm misalignment

[removed]

Figure 55 - First and full opening stress for rotational misalignment

5.5 Stress and strain in the connection

The plots and charts of the previous section provide insight into the general behaviour of the connection, but a closer look at the stress and strain in the connection is required to understand how it behaves under loads. These parameters can be visualized using contour plots. Alternatively, the values can be plotted against the load for a single point, investigating the behaviour for increasing loads.

Figure 56 - Von Mises stress equivalent. Left: MP flange. Right: TP flange

[removed]

Figure 57 - Plastic strain in the TP

The development of the plastic strain in the most deformed element in the dowel during the tensile load step is plotted in Figure 58. The plastic strain develops non-linearly with the load, especially after the connection starts to open. From this point on, an increasing fraction of the load is transferred by the dowel.

[removed]

Figure 58 - Plastic strain development in the dowel

5.5.1 A closer look at the dowel

To study this component more closely, a new model has been developed that removes most of the other parts to allow for a finer mesh. Only the dowel is modelled, with a fillet at the transition from the inclined plane to the vertical face of the dowel.

[removed]

Figure 59 - The mesh of the detailed dowel model

To incorporate realistic boundary conditions for the dowel, while still keeping the model complexity low, no hard degree-of-freedom limits are placed on the dowel. It is instead held in place by contact elements in a matching hole in a block with dimensions similar to the TP flange. This block is constrained. This method allows the dowel model to have an interface with a realistic stiffness. A distributed load is applied at the inclined plane. The magnitude of this load is taken from the pressure on the inclined plane at ULS load from the full sector model.

[removed]

Figure 60 - The detailed dowel model with load and boundary condition

[removed]

Figure 61 - Clockwise: x, y, z direction stress in lengthwise cross section for detailed dowel model

[removed]

Figure 62 - Equivalent plastic strain in the dowel

5.6 Fatigue assessment

All offshore structures are loaded by cyclic loading due to wind and waves. Therefore the fatigue limit state is often the governing failure mode for components of offshore structures. The resistance is typically determined with an S-N curve for the most critical fatigue detail. The intercept and slope of the S-N curves are given in codes for different structural details.

As the wedge connection is a fundamentally different concept from other types of connection, and the (partially) non-linear load-stress response due to the contact surfaces and preload, there is no obvious S-N curve to be used. Because of these uncertainties, it is recommended to perform experiments to develop such an S-N curve specifically for the various components of the wedge connection. Nevertheless, based on observations and results from the FE analysis, a qualitative assessment on fatigue can be performed at this stage by analysing the stress intensity.

Three main locations are identified as potentially particularly sensitive to fatigue: the shear plane in the dowel, the edge of the dowel-TP interface and the corner of the MP-TP interface (Figure 63).

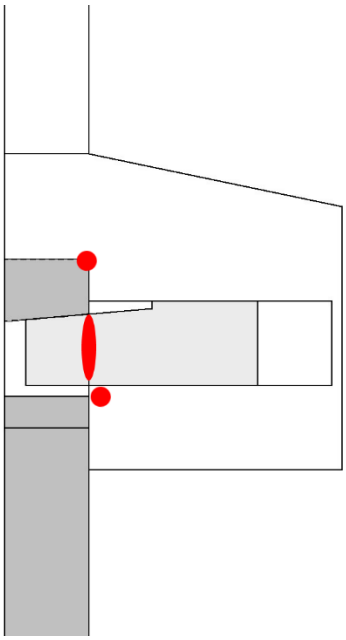

Figure 63 - Possible critical locations for fatigue

5.6.1 Non-opening of connection

[removed]

Figure 64 - Stress-gap plot for base case, with indicative tensile load ranges for the first 4 sea states.

As part of a previous graduation thesis that focussed on foundation design for offshore wind turbines, time series for wind and wave loading have been developed. These environmental loads are discretized into 18 sea states. The wind and wave loading are translated into bending moments at the connection elevation. These bending moments are combined with the axial load due to self-weight into a stress time history for each sea state. In an attempt to quickly visualize these loads, the minimum and maximum load, and the load range are plotted for each sea state against the probability of each sea state in Figure 65. The probability is calculated from an observed number of waves. shows that by far the most

waves occur in the first four sea states. The tensile stress ranges found for these four sea states are indicated in Figure 64 with vertical bars.

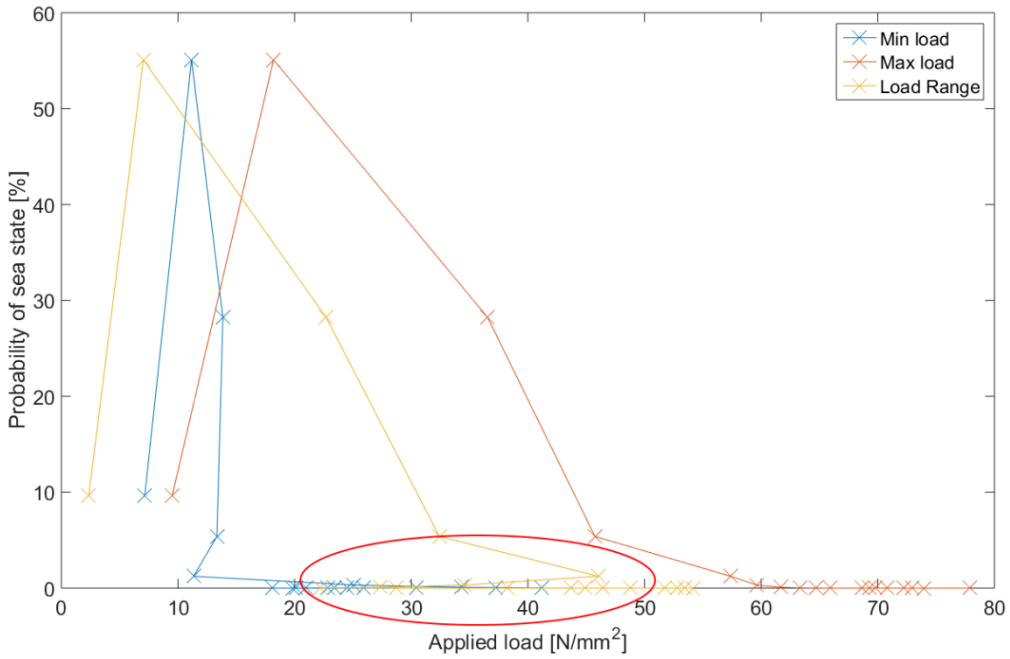

Figure 65 - Applied load vs. probability. Irregularity with higher sea states highlighted

5.6.2 Preliminary fatigue check of the dowel in shear

With the very conservative assumption that no load sharing takes place and the dowel transfers the full stress range in shear, the maximum shear stress range in the dowel can be calculated for each sea state from the maximum and minimum applied loads. This is purely analytical calculation, and does not take into account load transfer via preload.

To calculate the damage, a reference S-N curve is required. In DNV-RP-C203 (Det Norske Veritas 2010) an S-N curve is proposed for bolts loaded in shear:

$$\log(N) = 16.301 - 5.0\log(\Delta\sigma)$$

The damage over the lifetime can be calculated from the load stress ranges and the reference S-N curve with Miner's rule:

$$D = \sum \frac{N_{failure}}{n_{cycles}}$$

[removed]

Figure 66 - S-N curve from DNV, with stress range for different sea states

A more refined FE model, including contact surfaces and preload, with nodes at a number of locations interesting for fatigue could be loaded with stress ranges corresponding to the environmental loads. The actual stress ranges at those nodes can be extracted to develop an S-N curve, which can be compared to reference curves from literature. This would provide a first estimate of the fatigue life of the connection. Additionally, fatigue experiments will provide actual data on the performance of the connection.

6 Detailed design

Before the Wedge Connection can be realised, the design must be elaborated further. Based on the results of the FE study, discussions with industry experts and practical considerations for fabrication, installation and longevity of the connection the design is adapted. No detailed analysis is performed for these parts, as the FE results generally do not indicate any critical stresses in the affected areas. Including these details in the FE geometry would significantly complicate meshing and solving the model.

6.1 Materials

6.2 Structural details

Based on the results from the FE study, industry demands and fabrication concerns, a number of details are added to the dowel, MP and TP. Figure 67 shows the cross section of the connection system with these details added.

[removed]

Figure 67 - Detailed design in cross section

6.2.1 Design for fabrication

Fillets and chamfers are included at all right angles to facilitate fabrication.

6.2.2 Design for installation

[removed]

Figure 68 - Installation guides on the outside of the connection

6.3 Hydraulic system design

[removed]

7 Discussion

7.1 Interpretation of results

In this thesis the concept of the Wedge Connection has been developed from a first sketch to a detailed design with a solid performance in the ultimate limit state. A simple analysis based on free body diagram illustrates the principles of the connection. Introducing friction into the equations adds complication, as the magnitude of friction force cannot be expressed unless the components are experiencing relative motion. Furthermore, a major discussion can be had around the concept of expressing friction in a simple linear equation. Tribology literature is full of alternative models to improve simulation of real life friction. No such model was used for this investigation. Tribology seems to be too complicated to be captured in a compact set of design equations. To understand the frictional behaviour, application-specific experiments are required.

The dowel connection has two distinct load paths to transfer tensile loads from the TP to the MP. The first is by clamping the two flanges together with a preload that is generated through the inclined plane. The second is by loading the dowel itself in shear. The distribution between these two is dependent on their relative stiffness, which is difficult to estimate.

The preliminary design of the connection has undergone many different iterations before settling on the design with a single row of cylindrical dowels with a flat, inclined contact plane and an MP with a machined hole in-line with the axis of the MP and TP wall. This design was chosen for further analysis based on its relative simplicity and decent performance in initial FE models. The other versions of the connection are not necessarily discarded. The results found in the parameter study for generic items such as input pressure, friction coefficient and wedge angle are valid for other designs as well.

7.2 Recommendations for further research

The results from this thesis provide confidence in the concept of the wedge connection. Some additional details have already been proposed in chapter 0. It is recommended that the influence of these additions on the behaviour are investigated in a more detailed FE model.

As the connection is based on contact, friction is a critical factor in the design. In this investigation, friction was modelled as is common: with a single friction coefficient describing the relation between normal load and friction force. It is crucial to validate this model, and to perform experiments to determine the value of the friction coefficient for a number of candidate materials for the dowel and flanges. The experiment should be designed to closely replicate the geometry and loading of the connection.

Thanks to the modular design, the principle of the wedge connection can easily be tested with just a single sector. Such a test will take place in a simple tensile test bench. One important consideration for such a test is that a single sector does not provide any ring stiffness. This can be simulated by selecting appropriate boundary conditions and artificially increasing the radial stiffness, similar to the work of Lotsberg et al. (2012) for a grouted connection.

Offshore structures are subject to highly cyclic loading from wind and waves, often ensuring that fatigue life is the governing failure mode. A thorough investigation into the fatigue life of the complete structure is a major step to be taken in maturing the concept.

The non-linear nature of the connection complicates a fatigue life analysis, as the stress ranges cannot be simply extrapolated from one load level to another. Nevertheless, the fatigue life can probably best be estimated using the S-N curve method. This is also the industry standard. Separate runs of the FE model should be performed at different load levels to find the stress ranges.

8 Conclusion

The wedge connection has been developed in response to a number of perceived issues with other connection methods for offshore monopiles. Grouted connections have failed in the past and bolted connections are impractical to install below the waterline and require maintenance. In a comparison of these and a number of other new concepts, the wedge connection has shown to be favourable in terms of installation, serviceability, underwater application and scalability to larger diameters.

The core principle of the wedge connection is the inclined plane. This plane translates a horizontal hydraulic pressure into a vertical preload. This preload provides the primary load transfer path. A secondary load path is by loading the dowel in shear. At all contact planes, friction is present.

Based on this analytical model and the shear capacity of the dowel, a preliminary design was drafted for a reference 10 m monopile. A finite element model of the connection, taking into account non-linearity of the contact planes and material model was developed in ANSYS.

This model has been adapted and analysed with a number of different parameters. As expected, the friction coefficient proved to be crucial.

Overall, the wedge connection has proven to be a viable concept for offshore foundations. It allows for quicker, safer installation and more freedom in foundation design by applying the MP/TP connection under water.

9 References

4C offshore. 2013. “Monopile Support Structures.” *4C Offshore*, June 5, 2013. http://www.4coffshore.com/windfarms/monopiles-support-structures-aid4.html.

Blau, Peter J. 2001. “The Significance and Use of the Friction Coefficient.” *Tribology International* 34 (9):585–91. https://doi.org/10.1016/S0301-679X(01)00050-0.

Brown, Kevin H., Charles W. Morrow, Samuel Durbin, and Allen Baca. 2008. “Guideline for Bolted Joint Design and Analysis: Version 1.0.” Sandia National Laboratories.

Dallyn, Paul, Ashraf El-Hamalawi, Alessandro Palmeri, and Robert Knight. 2015. “Experimental Testing of Grouted Connections for Offshore Substructures: A Critical Review.” *Structures* 3:90–108.

Det Norske Veritas. 2010. “Fatigue Design of Offshore Steel Structures.” https://rules.dnvgl.com/docs/pdf/DNV/codes/docs/2010-04/RP-C203.pdf.

DNV GL. 2015. “Design of Offshore Steel Structures - DNVGL-OS-C101.” https://rules.dnvgl.com/docs/pdf/dnvgl/OS/2015-07/DNVGL-OS-C101.pdf.

European Commission. 2017. “Horizon 202 - Work Programme 2016-2017.”

European Committee for Standardization. 2005. “Eurocode 3: Design of Steel Structures - Part 1-8: Design of Joints.”

Gelder, Boudewijn van. 2016. “Double Slip Joint.”

GL. 2012. “Guideline for the Certification of Offshore Wind Turbines.” GL.

Gollub, Peter, Jacob Fisker Jensen, Dirk Giese, and Selcuk Güres. 2014. “Flanged Foundation Connection of the Offshore Wind Farm Amrumbank West - Concept, Approval, Design, Tests and Installation: Flanged Foundation Connection of the Offshore Wind Farm Amrumbank West - Concept, Approval, Design, Tests and Installation.” *Stahlbau* 83 (8):522–28. https://doi.org/10.1002/stab.201410178.

Henriksen, Erik Karl. 1973. *Jig and Fixture Design Manual*. New York: Industrial Press.

Holmberg, Kenneth, and Allan Matthews. 2009. *Coatings Tribology: Properties, Mechanisms, Techniques and Applications in Surface Engineering*. Tribology and Interface Engineering 56. Amsterdam: Elsevier.

Integrated Systems Research. 2008. “Optimizing Bolt Geometry for Fatigue Resistance.” http://www.kxinc.com/content/Kx%20Brochures/Bolted_Joint_Tech_Brief.pdf.

J. Van der Tempel, B Schipholt. 2003. “The Slip-Joint Connection.” Dutch Offshore Wind Energy Converter project.

KCI. 2015. “KCI’s Double Slip Joint.” *Offshore WIND* VI (02):37–41.

Kim, Jeong, Joo-Cheol Yoon, and Beom-Soo Kang. 2007. “Finite Element Analysis and Modeling of Structure with Bolted Joints.” *Applied Mathematical Modelling* 31 (5):895–911. https://doi.org/10.1016/j.apm.2006.03.020.

Kopeliovic, Dmitri. 2012. *Graphite as Solid Lubricant*. http://www.substech.com/dokuwiki/doku.php?id=graphite_as_solid_lubricant.

Lotsberg, Inge. 2013. “Structural Mechanics for Design of Grouted Connections in Monopile Wind Turbine Structures.” *Marine Structures* 32:113–135.

Lotsberg, Inge, Andrzej Serednicki, Andreas Lervik, and H\a akon Bertnes. 2012. “Design of Grouted Connections for Monopile Offshore Structures.” *Stahlbau* 81 (9):695–704.

Miyoshi, Kazuhisa. 2007. “Solid Lubricants and Coatings for Extreme Environments: State-of-the-Art Survey,” 2007. https://ntrs.nasa.gov/search.jsp?R=20070010580.

Nolle, H., and R. S. H. Richardson. 1974. “Static Friction Coefficients for Mechanical and Structural Joints.” *Wear* 28 (1):1–13. https://doi.org/10.1016/0043-1648(74)90097-0.

Pavlović, Marko, Christine Heistermann, Milan Veljković, Daniel Pak, Markus Feldmann, Carlos Rebelo, and Luis Simões da Silva. 2015. “Connections in Towers for Wind Converters, Part II: The Friction Connection Behaviour.” *Journal of Constructional Steel Research* 115 (December):458–66. https://doi.org/10.1016/j.jcsr.2015.05.009.

Ramsdale, Rob. n.d. “Coefficient of Friction Reference Table.” Engineer’s Handbook. Accessed March 16, 2017. http://www.engineershandbook.com/Tables/frictioncoefficients.htm.
Rolf de Vos. 2016. *FLOW - Competitive through Cooperation*. FLOW. http://www.flow-offshore.nl/images/flow-openbaar/FLOW_Book-11_EN.pdf.
Sabine Lankhorst. 2015. “ENECO: Update on the Grouting Issue of Princess Amalia Wind Farm.” *Offshore WIND*, December 10, 2015. http://www.offshorewind.biz/2015/12/10/eneco-update-on-the-grouting-issue-of-princess-amalia-wind-farm/.
Schaumann, P., and M. Seidel. 2000. “Failure Analysis of Bolted Steel Flanges.” In *7th International Symposium on Structural Failure and Plasticity (IMPLAST 2000)*. https://www.researchgate.net/profile/Marc_Seidel/publication/268201831_Failure_analysis_of_bolted_steel_flanges/links/55e3fdca08aecb1a7cc9e196/Failure-analysis-of-bolted-steel-flanges.pdf.
Schaumann, Peter, Rasmus Eichstädt, and others. 2015. “Fatigue Assessment of High-Strength Bolts with Very Large Diameters in Substructures for Offshore Wind Turbines.” In *The Twenty-Fifth International Ocean and Polar Engineering Conference*. International Society of Offshore and Polar Engineers.
Segeren, Maxim L.A., Tjeerd J.J. van der Zee, Eliz-Mari Lourens, and Apostolos Tsouvalas. 2014. “Investigation of a Slip Joint Connection between the Monopile and the Tower of an Offshore Wind Turbine.” *IET Renewable Power Generation* 8 (4):422–32. https://doi.org/10.1049/iet-rpg.2013.0163.
Seidel, M. 2014. “Substructures for Offshore Wind Turbines Current Trends and Developments.” *Festschrift Peter Schaumann*, 363–368.
Sif Offshore Foundations. 2017a. “Wind Foundations.” https://sif-group.com/en/wind/foundations.
———. 2017b. “Sif Awarded the Production of All Monopiles and Transition Pieces for EnBW’s Albatros Wind Farm.” https://sif-group.com/nl/nieuws/project-updates/403-nieuwe-opdracht-voor-sif-alle-mp-s-en-tp-s-voor-enbw-s-albatros-windpark.
Sika. n.d. “SikaGrout-3500 WP.” Accessed February 27, 2017. http://deu.sika.com/en/Windenergie/Windenergie/01a016/01a016sa04/01a016sa04200.html.
Sørensen, John Dalsgaard, and Jens N. Sørensen. 2010. *Wind Energy Systems: Optimising Design and Construction for Safe and Reliable Operation*. Elsevier.
Trelleborg. 2017. “Orkot TLM & TXM Marine Bearings.” 2017. http://tss-static.com/remotemedia/media/tss_orkot_marine/orkot_marine_pdf_s/literature/Marine_TXMM__TLMM_brochure.pdf.
Van Gelder, Boudewijn. 2017. “KCI Double Slip Joint Update.” Delft, October 5.
van Gelder, Klaas Boudewijn. n.d. In-line connection for an offshore onstruction; offshore construction; method for installing. European Patent Office EP 2 910 686 A2, filed February 25, 2015.
Veljkovic, Milan, Markus Feldmann, Johannes Naumes, Daniel Pak, Carlos Rebelo, and Luís Simões da Silva. 2010. “Friction Connection in Tubular Towers for a Wind Turbine.” *Stahlbau* 79 (9):660–68. https://doi.org/10.1002/stab.201001365.
Veljkovic, Milan, and Wylliam Husson. 2009. “High-Strength Wind Turbine Steel Towers.” HISTWIN.
Voormolen, JA, HM Junginger, and WGJHM van Sark. 2016. “Unravelling Historical Cost Developments of Offshore Wind Energy in Europe.” *Energy Policy* 88:435–444.
Wang, Erke, Thomas Nelson, and Rainer Rauch. n.d. “Back to Elements - Tetrahedra vs. Hexahedra.” Munich, Germany: CAD-FEM GmbH. Accessed March 30, 2017. http://www.designspace.com/staticassets/ANSYS/staticassets/resourcelibrary/confpaper/2004-Int-ANSYS-Conf-9.PDF.
White, H. S., and D. Zei. 1951. “Static Friction Tests with Various Metal Combinations and Special Lubricants.” *J. Res. Nat. Bur. Stand* 46:292–298.

WindEurope. 2017. “The European Offshore Wind Industry.” WindEurope.
Winer, Ward O. 1967. “Molybdenum Disulfide as a Lubricant: A Review of the Fundamental Knowledge.” *Wear* 10 (6):422–452.